László Mester

The new physical-mechanical theory of granular materials

2009

Contents

Introduction ……3
Granular material as a distinct state of matter ……4
Physical properties of the granular material in relation to the different states of matter ……6
Granular material as a state of matter ……10
Physical-mechanical basic laws of the non-cohesive granular materials ……14
Law I ……15
Law II ……15
Law III ……17
Law IV ……24
Stresses in the non-cohesive granular materials ……26
Active stress state ……31
Development of the active stress state ……31
Pressures acting on the vertical retaining wall ……36
Arch formation of granular materials ……39
Condition of the arch formation ……39
Character of the discharge ……44
Mechanism of the arch formation ……46
Geometric equation of the arch ……47
Principle of the hopper design ……50
Experimental results ……53
Stresses in cohesive granular materials ……55
Lateral pressure ……55
Inclination angle of the free slope ……59
Active stress state ……64
Summary ……69
Bibliography ……73

Introduction

Following Coulomb's and later Rankine's work the physical-mechanical theoretical research of granular materials has been characterised by the use of stress analysis deduced for solids since the 18th century. Others seem to detect the characteristic features of viscous liquids in granular materials, therefore they describe the physical behaviour of granular materials using the laws pertinent to viscous fluids. In my opinion most of the theorems, which were put for cotinuums, cannot be applied to the aggregation of separate, solid granules. Only those natural laws can be considered as the starting point of examination, which are also valid for the universal material.

This work – breaking away from the previous tradition – would like to approach the physical mechanical properties of granular materials from a new point of view. As a result, the critical analysis of theories formulated earlier in this research area is not the objective of this paper, since the new principles were laid down irrespective of those hypotheses. Contrary to the continuum theory, by examining the equilibrium and kinetic state of individual granular particles this new thesis is based on simple experiments, on the Newtonian laws, and on an empirical law, the law of friction.

Granular material as a distinct state of matter

The physical appearance of materials found in nature is quite varied. The most substantial part of the Earth's surface is covered by oceans, seas, lakes, that is to say, covered by water. The dry land is more diverse: one can find rocky mountain ridges, surfaces covered by gentle slopes and deserts with sand dunes. In places the earth is covered by snow or ice in winter. Above the surface level the wind is blowing, or we can experience a period of calm, that is to say we can feel the air. The sun is shining above us and we know that inside the sun one would find another state of matter. The outward form of the water that covers substantial part of the Earth is in itself diverse. At normal temperature and pressure water is liquid, but with the increase of temperature it evaporates more and more quickly, and it turns into water vapour. Fog or clouds form. When water vapour freezes, and precipitates in cold, then snow falls, and it condenses into a granular material. When snow melts, the result is liquid, which in turn becomes solid when it freezes. That is to say water can exist in liquid, vapour (gas), snow (granular) and ice (solid) states. In each of its phases water has different physical properties, and behaves conforming to different laws.

Physics differentiates among the most prominent forms of appearance of material by classifying them into the different states of matter: plasma, gas, liquid and solid Some material cannot be put strictly under one category, because they bear the physical properties of two or more states of matter. These materials, however, can be described by applying the laws pertaining to materials in a similar state of matter.

Granular material cannot be put under any one of the above mentioned four categories. Furthermore the physical-mechanical properties of granular material do not make it possible to describe its behaviour successfully using the physical laws of one or more phases.

A granular material is a conglomeration of large number of solid particles related to one another, where the granules – as the constituent of the aggregate – in spite of the affecting forces retain their form, and the incidentally arising cohesive force between the granules is substantially smaller than the inner cohesion of the individual granules.

The overall, coherent physical system of granular material has not been set up yet, scientific analysis is available only for a few prominent, primarily soil mechanical problems. Several theories have been applied for the handling of these problems, which speculations, however led to contradictory results. Furthermore no connection resting on firm, uniform physical foundations exists between the theories, or if there is a relation, it is disputable. The majority of mechanical theories dealing with granular materials apply the method of stress analysis deduced for solids, which procedure presupposes, that the granular material is a solid phase continuum.

There are theories, according to which granular materials can be approached with the laws pertaining to viscous liquids, since granular material exhibits viscoelastic and viscoplastic properties. Although, the difficult theoretical notions provide an approximate solution to individual mechanical problems, they cannot be applied to an overall, reliable description of granular material behaviour.

The opinions concerning the state of matter of granular materials are not unanimous. This is reflected in the fact that granular material does not have a single uniform name, for example the following designations: scattering, powderlike, loose, granulated, grainy, particulate, granular and gritty are all used.

The physical behaviour and properties of granular materials exhibit substantial qualitative difference from the materials in other states of matter, and should therefore be considered an additional state of matter in its own right

The idealised notion of granular material makes the simplified explanation of its physical behaviour, properties and origin possible, similarly to the hypotheses applied to perfect gases, ideal liquids and crystalline solids. The ideal granular material is a conglomeration of large number of solids (granules) where the mass of the solid particles is small compared to the mass of the material, in this aggregate attractive force does not operate between the particles, Coulomb friction rule governs them.

Physical properties of the granular material in relation to the different states of matter

The basis for classification according to states of matter depend on the question whether the material can hold its own shape and volume or not. The basic criteria of classification of the three classical states of matter are the following:

- gases: have no definite shape or volume;
- liquids: have no definite shape, but have definite volume
- solids: have definite shape and volume.

Regarding the question of definite shape and volume it is the characteristic of the granular material that:

- In part it has definite shape, the granular aggregate holds its shape in the angle of repose, but under this angle it takes the shape of its container. This attributive places the material between liquids and solids.
- In part it has definite volume, but it can be compressed to a limited extent. The compressibility of granular materials stands between the compressibility of gases and solids.

The researches on substance structure concerning the states of matter found that the determining factors in the question whether a material holds a definite shape or volume lie in the physical properties of its constituents and the nature of interaction between these particles. For this reason modern physics studies the kinetic state of the smallest particles attributed to the material, their relative position and the particle interaction when defining the different states of matter. This made it possible that in

natural science, in addition to the three classical states of matter, a fourth state of matter, was accepted, the plasma state.

It seems to be necessary to emphasise the expression smallest constituent characteristic of the material, since it is of primary importance in the definition of the different states of matter. Consequently

- A material in *plasma* state consists of the disintegrated parts of molecules or atoms, the molecule ions or atomic ions. The plasma state is characterized by the interactions of atomic or molecule ions and electrons, and not by the other parts of the atom or molecule.
- The physical properties of a material in the *gas state* are determined by the interactions of gas molecules – in case of noble gases the interactions of atoms.
- Regarding *liquids* the determining factors are again the movements of the atoms or molecules, and the nature of relation between them. In the case of water it is the interactions of H_2O molecules and not the hydrogen or oxygen atoms, or the water drop, which characterize the liquid.
- In the case of crystalline *solids* the physical properties of a material in the solid state can be explained with the nature of interaction of the atoms, molecules or ions positioned in the lattice nodes of a crystal structure, and cannot be described for example with the interactions of elemental crystals and crystallites, or with the individual properties of the atoms and its parts, which constitute the molecules positioned in the lattice points.
- In the case of *granular* material the smallest constituent characteristic of the material is the granule. The atomic particles, the atoms and molecules that constitute the granules, are not direct characteristics – at least in physics they cannot be regarded as significant physical properties– of a material, just like as in the case of gases and liquids, where material is not characterised by the atomic particles, which constitute the atom or molecules, or by the individual physical properties and interactions of atoms either.

The most significant characteristics of the three classical states of matter can be summarised in the following way:

Gaseous state: The molecules of gases – in case of noble gases the gas atoms – move freely in the space available for them, they collide elastically with one another in a random motion. The average distance between the constituting particles of gases is relatively big in proportion to their size, the intermolecular forces between the particles are very weak. In the case of ideal gases intermolecular force can be disregarded. Molecules move with a translational, rotational and vibrational motion. Gases evenly fill the space available for them, that is to say they have no definite shape or volume.

Liquid state: The intermolecular forces between the smallest constituents characteristic of liquids, between the atoms or molecules are strong enough to prevent the particles moving away from each other as a consequence of thermal motion, but not strong enough to prevent their change of position. Compared to gases, the translational motion of the molecules are smaller, while they also carry out rotational and vibrational movement. Due to their motion and proximity the constituting particles collide elastically with one another all the time, thus touch one another, therefore liquids have a definite volume. The force of attraction between the particles is so small compared to the Earth's gravitational force that it is not enough for individual shape formation, as a result liquids have no definite shape.

Solid state: The smallest constituting particles, characteristic of solids are the atoms, molecules or ions. Their position is fixed and geometrically determined in a crystalline structure, particles carry out only vibrational motion. The intermolecular forces are strong, which prevent their permanent displacement from their state of equilibrium. As a result solids have definite shape and volume.

Granular material exhibits significant differences from the aggregational properties of the three classical states of matter. The constituents of an ideal granular material, the granules are at a relative rest. There are no forces of attraction between the particles, the material is kept in an aggregate by the compressive forces originating from the gravitational force, by the shear forces arising on the surface of the granules, and by the static friction force. Due to these forces the ideal granular material remains stable until the angle of repose is reach, thus it has only partly a definite shape. The constituting particles are in constant contact, therefore in

quiescent state granular material has definite volume. Under pressure the material is compressed, the granules take up a more efficient space filling position. The compressibility of granular material is small compared to gases, but it is big in comparison to solids.

The physical properties of ideal granular material exhibit the following significant differences in characteristics compared to the features of other states of matter:

- In contrast to *gaseous state:* the constituting particles are in constant contact with each other, and it has definite volume;
- In contrast to *liquid state:* granular material has in part a definite shape;
- In contrast to *gaseous and liquid state:* The constituting particles are in a relative collision free, quiescent state and static friction force – shear force – arise in them;
- *Solid state:* there is no attractive force between the constituting particles, therefore granular material has only in part a definite shape.

Granular material exhibits such qualitative differences concerning the most substantive characteristics of the different states of matter that its definition as a separate state of matter in its own right becomes justified.

The brief, straight to the point definition – with no pretence to completeness – of the idealised case of the states of matter is the following.

Perfect gas: disordered aggregate of molecules (in case of noble gases atoms) with no intermolecular forces, where the molecules move far apart from each other, undergoing random elastic collisions.

Ideal liquid: Aggregate of molecules moving close to each other, undergoing constant elastic collisions.

Crystalline solid: The ordered aggregate of vibrating atoms, molecules or ions, which are fixed in their structure with great force.

Ideal granular materials: the aggregate of relatively static particles, which are in constant contact with each other, in this assembly the force between the constituting particles is composed of the compressive force arising from the gravitational force and of the friction force, which is proportional to it, there is no cohesion force between the particles.

The notion of granular material, as a separate state of matter is primarily important from a mechanical viewpoint. (The basis for categorization into different states of matter has a mechanical origin: the reason for having a definite shape or volume can be deduced from the intermolecular forces between the constituting particles.) The mechanical properties of the different states of matter show distinctive, substantial differences:

- *gases* respond to an increase in pressure with the significant reduction of their volume (at constant temperature the multiplication product of volume and pressure is constant), therefore they can withstand compressive stress only in part, at the expense of volume change. In perfect gases there is no attractive force between the constituting particles, therefore no tensile stress can arise in the material. In static – not flowing – gases no shear stress arises.
- *liquids* has small compressibility, from a mechanical point of view they can be regarded incompressible, therefore they can withstand compressive stress. The intermolecular forces are strong enough to prevent the constantly colliding molecules from moving far away from one another. The state of equilibrium or stability can only be attained under a given outside pressure, that is to say, from a mechanical standpoint a liquid cannot withstand tensile stresses. (When the pressure is around p=0 the liquid breaks up, its molecules fly apart and turn into gaseous state) There is no friction in ideal liquids, in real liquids static friction does not arise either.
- *solids* can be regarded as incompressible, the constituting particles join together with great force, therefore they can withstand tensile, compressive and shear stress.
- ideal *granular* material has small compressibility, therefore it can withstand compressive stress. In the non-cohesive granular materials only shear stress arises in addition to compressive stress, no tensile stress manifests itself.

Granular material as a state of matter

The notion that granular material must be regarded as a separate state of matter can be justified not only because its distinct physical properties, which differentiate it

from other states of matter, but also because granular material is one of the existing outward forms of raw material, that is to say it is one of defined states of matter.

Granular material – as the conglomeration of large number of solids, where the constituting solids are small in proportion to the total mass of the material – generally comes into being when large-sized solids are mechanically cut up, or when the solids themselves break up into smaller pieces. Its formation, that is to say, the bringing of the material into a granular state can be achieved not only in a mechanical way, as it is also true for the granular materials in nature, which were formed not exclusively by mechanical disintegration either. Granular material can be produced via a thermodynamic method.

It is known, that if the kinetic energy of the molecules of a liquid exceeds a threshold it changes into gaseous state and if it goes below another threshold the liquid turns into solid and the process of crystallization begins. The threshold values of the thermodynamic state parameters characteristic of the different states of matter can be illustrated in a p – t (pressure-temperature) diagram. In Figure 1 the p – t diagram of H_2O can be seen.

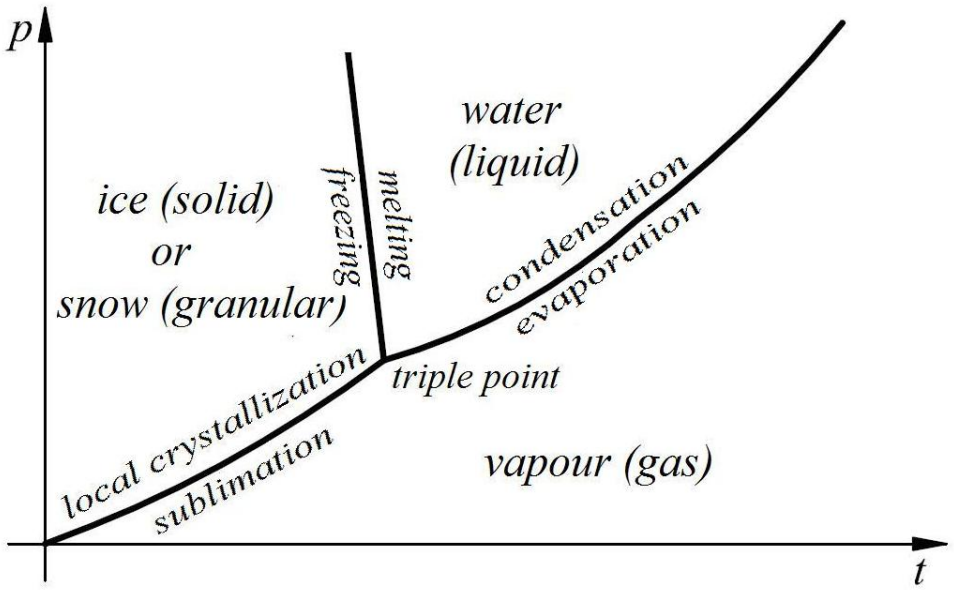

Figure 1. p-t diagram of H_2O

The curve that joins the triple point and the origin of the p – t diagram is called the sublimation curve. The material passes from the solid ice phase into the vapour phase of the gas state by for example pressure reduction and by the crossing of the sublimation curve. Crossing the sublimation curve backwards, from vapour phase granular snow is formed not ice. The granular material – in case of water, the snow – comes into being as a result of crystallization in the local clusters. The process can be called *local crystallization*, the physical explanation of which lies in the phenomenon that the molecules which move with slow translational motion (under low temperatures) cannot leave the attraction field of the van der Waals type forces – for example as a result of heat loss – therefore the translational motion of the molecules ceases.

The molecule pair - bonding the new molecules, which collide into them - form a crystal lattice, the growing crystals then bring about the granules. The density of molecules in the gaseous state is very low in comparison to the molecular density of the solid state, therefore the local crystallization processes, which are relatively far from one another bring about the multitude of separate granules, which after having precipitated form a granular conglomeration.

Under constant temperature the process of getting from gas phase to granular phase is accompanied by heat loss, which is the sum of the melting and the evaporation heat.

The states of matter change at the phase boundaries of the p – t diagram. If the matter crosses the sublimation curve from the solid phase toward the gas phase, we will get a gas, however changing the direction crossing the curve from the gas phase we will obtain a granular material. Thus the states of matter, in compliance with the direction of crossing the phase boundaries are the following:

gas → local crystallization → *granular* → melting → *liquid* → evaporation →*gas;*

nevertheless, from the other direction:

gas → condensation → *liquid* → freezing → *solid* → sublimation → *gas*.

From granular phase to solid phase we can get by crossing the same phase boundary twice:

granular → melting → *liquid* → freezing → *solid*.

Granular material can be produced directly from liquid phase if we place a multitude of crystal nuclei - which are approximately at an equal distance from one another - into a supercooled liquid at the same time. The crystal growth is hindered by the neighbouring crystals, whose geometric crystal position is not symmetrical or congruent, therefore no or only occasional lattice forces develop between the crystals, the inner cohesive force of the individual granules are substantially greater than the incidental cohesive forces acting between the granules.

The substantial physical properties of the granular material differ significantly from the characteristics of those materials whose chemical properties are identical, nevertheless belong to the solid, liquid or gaseous state. Its volume weight, its refractional, thermodynamical, acoustic, electric and mechanical properties and behaviour, and the fact that most material can be brought into granular state justifies the classification of the granular material as a distinct state of matter by its own right.

Basic physical-mechanical laws of the non-cohesive granular materials

I. In the non-cohesive granular materials only compressive and shear stresses can develop.

II. In the non-cohesive granular materials at a quiescent state the stresses developed by the vertical-direction compressive stresses act downwards in the $\pm 90^0 - \varphi$ zone measured from the vertical direction. (φ is the angle of friction of the material.)

III. The value of the lateral pressure rising from the self-weight of the non-cohesive granular material is ($\frac{h\gamma}{2}$), the half of the product of the depth (h) and volume weight (γ), its direction deviates from the horizontal downwards with the angle of friction developed in the material, if the surface is horizontal and over the given depth the material fills the space evenly closing an angle φ with the horizontal.

IV. The non-cohesive granular materials conform to the physical-mechanical laws characteristic of them until their constituting elements, the grains keep their relative quiescent state. When the grains go into motion – collide with each other -, the granular materials behave according to the physical-mechanical laws of the liquids.

The physical-mechanical laws of the non-cohesive granular materials prevail with a statistical character, because the material itself consists of a multitude of different grains.

Law I

Law I is the physical-mechanical definition of the non-cohesive granular materials.

In ideal liquids only compressive stresses develop, the non-cohesive granular materials are capable of withstanding compressive and shear stresses, while solids are capable of bearing compressive, shear and tensile stresses. The non-cohesive granular materials differs from the solids in the respect that they are not capable of withstanding tensile stress, and they are distinct from the ideal liquids because shear stresses also develop in them. At the same time the components of the liquids are in constant relative motion – collide with each other -, while the components of the granular materials, the grains are in a relative quiescent state.

Law II

Law II formulates the direction of the spreading of the vertical compressive stresses. The natural stability of the free slope provides its experimental proof (Figure 2).

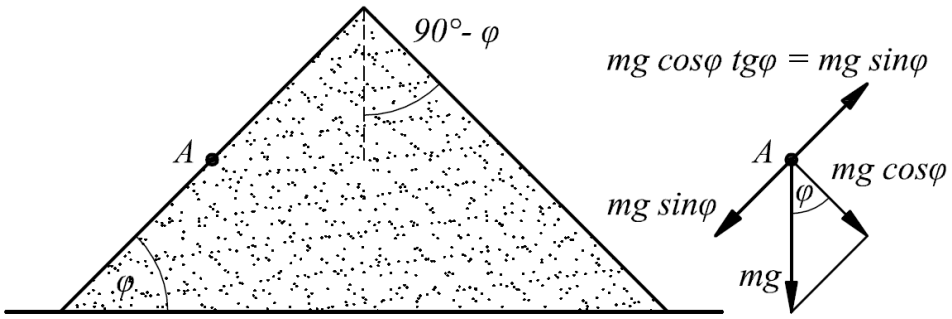

Figure 2. The boundary equilibrium position of the grain located on the side of the slope

In the conglomeration of grains the self-weight of the grains produces the vertical compressive stress. If a stress vector acted on the grain marked *A* located on the side of the slope– in boundary equilibrium position - inclined at an angle of more than $90^0 - \varphi$ from the vertical then the grain would loose its equilibrium position and slide down.

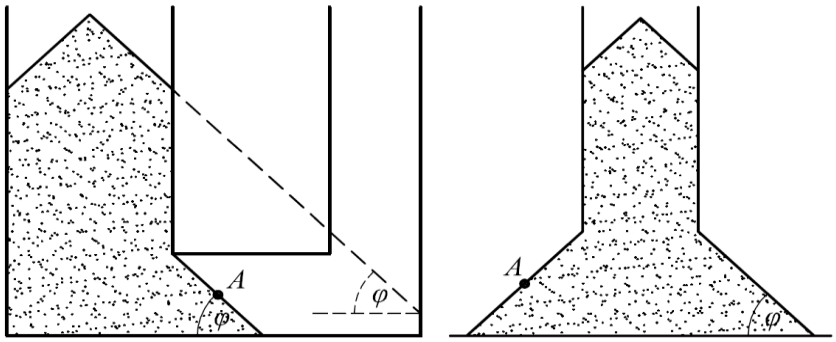

Figure 3. The stresses developed by the vertical compressive stresses incline at an angle bigger than φ to the horizontal.

Further experiments prove the correctness of the Law II (Figure 3). If a compressive stress making a smaller than φ angle with the horizontal acted on the grain marked *A*, the angle of inclination angle φ of the natural slope would be smaller than φ. If the vertical compressive stress induced, for example, a horizontal stress, it would thrust down the grains located on the side of the slope. The material would spread and would take a kind of shape that is illustrated in Figure 4. However, it does not exist.

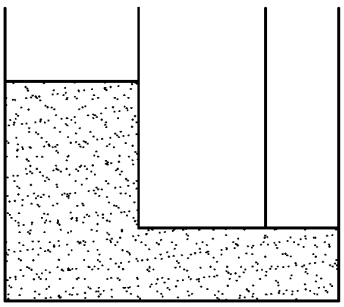

Figure 4. If the compressive stresses induced horizontal stresses, this would be the position of the granular material.

Law III

In the cases described in the Law III the lateral pressure is $\frac{h\gamma}{2}$, and its direction inclines from the horizontal downward with the angle of friction rising in the inside of the material. Its proof is as follows:

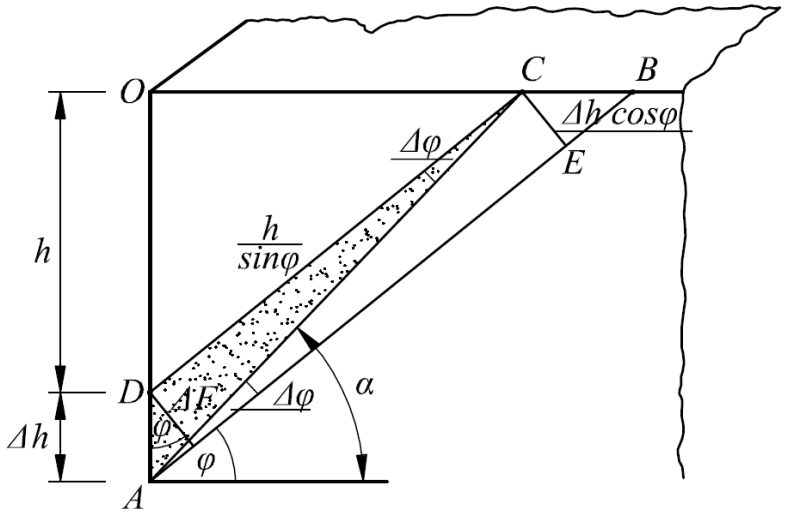

Figure 5. Infinite Quadrant of the Horizontal Terrain

Figure 5 shows that part of the non-cohesive granular material aggregate of infinite-expansion and horizontal-terrain, which is cut out theoretically by two vertical planes perpendicular to each other, (consequently, it shows an infinite quadrant of the horizontal terrain,) which makes the planar execution of the mechanical tests possible. According to the Law II, from the material part under the section *AB* only reaction stresses produced by the material part over the plane *AB* can act on the plane *OA*. If we took off the granular material located in the triangle *OAB*, then the material would remain stable in the natural angle of repose *AB* inclining at an angle φ to the horizontal. On the plane *OA*, stresses can only rise from the self-weight of the granular material located in the space part *OAB*. On the plane *AB* an equilibrium boundary position exists; the material having a friction coefficient of $\mu = tg\varphi$ does not slide as yet on the slope with an inclination of angle φ. If we increased the slope angle with $\Delta\varphi$ of a very low value, then the material above it could slide down with

constant acceleration on the slope with the inclination angle $\varphi + \Delta\varphi$, i.e. it would exert a force in direct proportion to its mass and acceleration on the plane *OA*. Due to the physical properties of the granular materials there are infinitely many slopes with an inclination angle $\varphi + \Delta\varphi$, above which angle, on the slopes increased by the angle $\Delta\varphi$, the weight of the materials exerts slope-direction stresses on the plane *AO*. According to Figure 5, on the slope with an inclination angle of $\alpha = \varphi + \Delta\varphi$, produced as a result of the depth increased by *Δh,* the granular material *ADC* weighs heavily on the slope with its self-weight (*ΔG*) and with the weight of the material located above it (*G*). The material amount *ADC* is supported on section *Δh*. The projection of the surface section *Δh,* perpendicular to the slope is $\Delta F = \Delta h \cdot \cos(\varphi + \Delta\varphi)$. Considering that the *Δh* is very little, therefore, the stress distribution can be considered even, so it can be stated for the slope-direction stress developed there:

$$\sigma_\alpha = \frac{(G + \Delta G)(\sin\alpha - \mu\cos\alpha)}{\Delta F},$$

In the unit-length space part

$$G = \frac{h^2\gamma}{2} ctg\,\varphi,$$

and

$$\Delta G = \frac{1}{2} \cdot \frac{h\gamma}{\sin\varphi} \Delta h \cdot \cos\varphi,$$

that is,

$$\Delta G = \frac{h\gamma}{2} \Delta h \cdot ctg\,\varphi,$$

furthermore,

$$\Delta F = \Delta h \cdot \cos(\varphi + \Delta\varphi).$$

The $(\sin\alpha - \mu \cdot \cos\alpha)$ in the equation can also be expressed:

$$= \sin(\varphi + \Delta\varphi) - tg\,\varphi \cdot \cos(\varphi + \Delta\varphi),$$

$$= \sin\varphi \cdot \cos\Delta\varphi + \cos\varphi \cdot \sin\Delta\varphi - \frac{\sin\varphi}{\cos\varphi}(\cos\varphi \cdot \cos\Delta\varphi - \sin\varphi \cdot \sin\Delta\varphi),$$

$$= \cos\varphi \cdot \sin\Delta\varphi + \frac{\sin^2\varphi}{\cos\varphi}\sin\Delta\varphi,$$

$$= \frac{\sin\Delta\varphi}{\cos\varphi}(\cos^2\varphi + \sin^2\varphi),$$

$$= \frac{\sin\Delta\varphi}{\cos\varphi}.$$

Substituting the values of the *G*, *ΔG*, *ΔF* and $\sin\alpha - \mu\cdot\cos\alpha$ into the relation written for the σ_α:

$$\sigma_\alpha = \frac{\left(\frac{h^2\gamma}{2}ctg\varphi + \frac{h\gamma}{2}\cdot\frac{\Delta h\cdot\cos\varphi}{\sin\varphi}\right)\frac{\sin\Delta\varphi}{\cos\varphi}}{\Delta h\cdot\cos(\varphi+\Delta\varphi)},$$

$$\sigma_\alpha = \frac{\frac{h\gamma}{2}ctg\varphi(h+\Delta h)\frac{\sin\Delta\varphi}{\cos\varphi}}{\Delta h\cdot\cos(\varphi+\Delta\varphi)},$$

$$\sigma_\alpha = \frac{h\gamma}{2}\cdot\frac{\frac{\cos\varphi}{\sin\varphi}(h+\Delta h)\frac{\sin\Delta\varphi}{\cos\varphi}}{\Delta h(\cos\varphi\cdot\cos\Delta\varphi - \sin\varphi\cdot\sin\Delta\varphi)},$$

$$\sigma_\alpha = \frac{h\gamma}{2}\cdot\frac{h+\Delta h}{\Delta h\cdot\sin\varphi\left(\cos\varphi\frac{\cos\Delta\varphi}{\sin\Delta\varphi} - \sin\varphi\right)},$$

$$\sigma_\alpha = \frac{h\gamma}{2}\cdot\frac{h+\Delta h}{\frac{\Delta h\cdot\sin\varphi\cdot\cos\varphi}{tg\Delta\varphi} - \Delta h\cdot\sin^2\varphi},$$

but the $tg\Delta\varphi$ can be expressed from the triangle *ACE* of Figure 5:

$$tg\Delta\varphi = \frac{\Delta h\cdot\cos\varphi}{\frac{h}{\sin\varphi} + \Delta h\cdot\sin\varphi},$$

$$tg\Delta\varphi = \frac{\Delta h\cdot\sin\varphi\cdot\cos\varphi}{h + \Delta h\cdot\sin^2\varphi},$$

therefore,

$$\sigma_\alpha = \frac{h\gamma}{2}\cdot\frac{h+\Delta h}{\frac{\Delta h\cdot\sin\varphi\cdot\cos\varphi}{\frac{\Delta h\cdot\sin\varphi\cdot\cos\varphi}{h+\Delta h\cdot\sin^2\varphi}} - \Delta h\cdot\sin^2\varphi},$$

$$\sigma_\alpha = \frac{h\gamma}{2}\cdot\frac{h+\Delta h}{h+\Delta h\cdot\sin^2\varphi - \Delta h\cdot\sin^2\varphi},$$

$$\sigma_\alpha = \frac{h\gamma}{2} \cdot \frac{h + \Delta h}{h},$$

$$\sigma_\alpha = \frac{h + \Delta h}{2}\gamma,$$

if the Δh is very little, that is Δh → 0, then α → φ, consequently $\sigma_\alpha \rightarrow \sigma_\varphi$, i.e. the direction of the stress inclines at an angle φ to the horizontal. Consequently,

$$\lim_{\Delta h \to 0} \sigma_\alpha = \frac{h\gamma}{2},$$

that is,

$$\boxed{\sigma_\varphi = \frac{h\gamma}{2}}.$$

As a result of the deduction it can be established that the stress distribution is linear against the depth.

However, in case of granular materials one cannot speak of a stress in the classical sense, since the force effects are transmitted at the contact points of the granules, i.e. from one point to another, not on a surface perpendicular to the given direction. Not on a surface, because the material is a discontinuum and the grains touch each other only at points. Therefore, the meaning of the stress can be interpreted as the average force imparted to one surface and these average forces are transferred from one granule to another. The direction and size of these forces manifest themselves as a statistical average on a given surface.

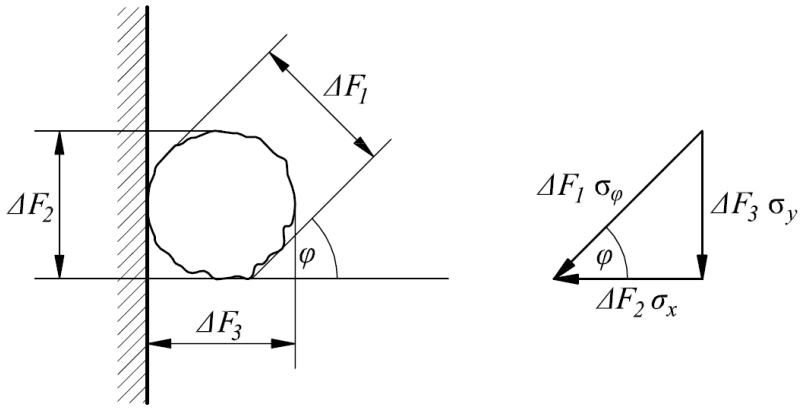

Figure 6. Division of the average force acting on the grain located next to the wall into a horizontal and a vertical component

Let us examine what the magnitude of the force is, which the above deduced stress σ_φ, inclining at an angle φ to the horizontal, exerts on a vertical wall. Through the contact points force arrives from the neighbouring granules at the grain –which is supported by a frictionless vertical wall – shown in Figure 6. The resultant of this force effect should be equal with the product of the stress σ_φ calculated for the surface ΔF_1, i.e. considering its magnitude and direction the compression force acting on this grain corresponds to the statistical average of the force exerted at this depth in the given granular material. This granule presses the vertical frictionless wall with a horizontal $\Delta F_2 \sigma_x$ force on the wall section ΔF_2 at the contact point. The vertical-direction force $\sigma_y \Delta F_3$ is received by the grain or grains located under it. The surface of sections ΔF_1, ΔF_2 and ΔF_3 are equal surfaces on statistical average, because, considering their shape and position, the grains are spheres on statistical average; the projections of the spheres from any direction are of equal surface area. (If a granular material – for example, rice – consists of oblong grains; considering the random arrangement of the grains the average of their projection taken in any direction is a circle, i.e. the grains must be considered as spheres on statistical average.)

Consequently, it can be written for the vector triangle of the Figure 6

$$\sigma_x \Delta F_2 = \sigma_\varphi \Delta F_1 \cos\varphi ,$$

but since

$$\Delta F_1 = \Delta F_2 ,$$

therefore

$$\sigma_x = \sigma_\varphi \cos\varphi .$$

It comes from the result of the above consideration that *in granular material the stresses* – the average forces calculated for a given surface – *can be decomposed or added as vectors.* From the $\sigma_x = \sigma_\varphi \cos\varphi$ equation the factor of static pressure is received after the $\lambda = \dfrac{\sigma_x}{\sigma_y}$ substitutions, that is

$$\sigma_y = h\gamma \qquad\qquad \sigma_x = \frac{h\gamma}{2}\cos\varphi ,$$

so

$$\boxed{\lambda = \frac{\cos\varphi}{2}}.$$

Up to this point, only the shear stresses generated by the stresses acting perpendicularly to the direction inclining at an angle φ to the horizontal and rising from the self-weight were taken into account at the deduction of the static pressure. The shear stresses τ_y, produced by the horizontal stress components - $\sigma_x = \frac{h\gamma}{2}\cos\varphi$ - reduce the vertical stresses $h\gamma$ with $\tau_y = \frac{h\gamma}{2}\cos\varphi \cdot tg\varphi$,

that is

$$\tau_y = \frac{h\gamma}{2}\cos\varphi\frac{\sin\varphi}{\cos\varphi},$$

so

$$\tau_y = \frac{h\gamma}{2}\sin\varphi.$$

Considering that the stresses σ_φ act in pairs on the theoretic plane *OA* assumed inside the granular material (Figure 5), therefore, the vertical-direction stresses $h\gamma$ are reduced by $2\tau_y$, consequently

$$\sigma_y = h\gamma - 2\tau_y,$$

that is

$$\sigma_y = h\gamma - 2\frac{h\gamma}{2}\sin\varphi,$$

and

$$\sigma_y = h\gamma(1-\sin\varphi).$$

Consequently, the figure of the stresses acting inside the non-cohesive granular materials at quiescent state can be constructed (Figure 7).

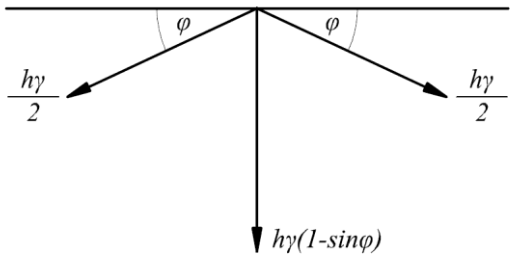

Figure 7. Stresses acting at a quiescent state

If the plane *OA* according to Figure 5. is a theoretic plane assumed inside the granular material, then the angle of friction is φ there. In this case a compressive stress of σ_φ, inclined at an angle φ to the horizontal acts on both sides of the plane *OA* (Figure 7.). On the plane *OA* the σ_φ's can be divided into horizontal and vertical components (Figure 8.). The horizontal components have the value

$$\sigma_x = \frac{h\gamma}{2}\cos\varphi,$$

they are perpendicular to lane *OA* and satisfy the action-reaction law. The vertical stress components of σ_y complement the vertical stresses to $h\gamma$ symmetrically to plane *OA* in a reciprocal way.

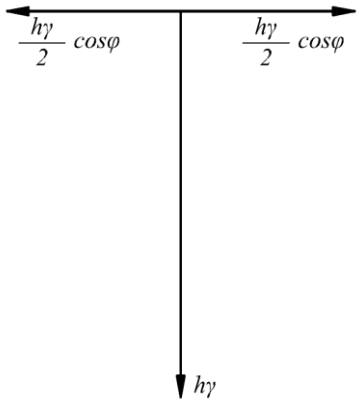

Figure 8. The horizontal and vertical stress component at a quiescent state

If the plane *OA* according to Figure 5 is a frictionless wall, then that is capable of taking only horizontal stress, i.e. the horizontal component of the σ_φ, which is

$$\sigma_x = \frac{h\gamma}{2}\cos\varphi.$$

At the same time the vertical component of the σ_φ complements the vertical stress component of the material *OAB* to $h\gamma$.

If the plane *OA* is an actual rough, rigid wall, which serves to support the *OAB* material amount, then the development of the static pressure can be interpreted as follows.

After filling up the *OAB* material amount behind the *OA* wall the value of the $\sigma_\varphi \frac{h\gamma}{2}$ is not reached immediately, since due to the inclined stress effect and because of the friction rising on the wall a weight force intake is realised on the plane *OA*. As a result of the weight-force intake the force acting on the plane *AB* is reduced; so it is not capable of producing stresses with the value of $\frac{h\gamma}{2}$ and in the direction *AB*. The freshly filled-in material comes to a standstill by finishing its consolidation motion. As a result of the quiescent state the friction rising on the wall is reduced to zero, consequently the stresses σ_φ are decomposed into their horizontal and vertical components. In the *OAB* material the vertical components complement the vertical stress components to $h\gamma$, and supplement the weight of the *OAB* material to $\frac{h^2\gamma}{2} ctg\varphi$. At this time the horizontal component of stress σ_φ acts on the *OA* wall. Consequently the horizontal component of the static pressure is:

$$\sigma_x = \frac{h\gamma}{2}\cos\varphi,$$

and, therefore the factor of static pressure is (λ):

$$\boxed{\lambda = \frac{\cos\varphi}{2}}.$$

Law IV

Law IV can be proved experimentally.

As a result of the experiment demonstrated in Figure 9, due to the collision of the grains, the granular material behaves according to the laws of the communicating vessels.

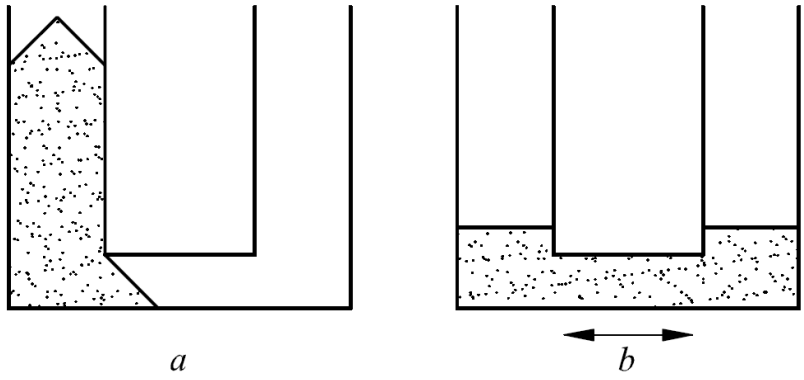

Figure 9. a) state of rest b) state formed as a result of vibration

In Figure 10 as a result of the vibration, and due to the collision of the grains the body with bigger volume weight γ_1 and the body with smaller volume weight γ_2, - which were place into the granular material with volume weight γ - sinks to the bottom of the vessel, or floats on the surface of the granular material respectively; consequently the law of Archimedes prevails.

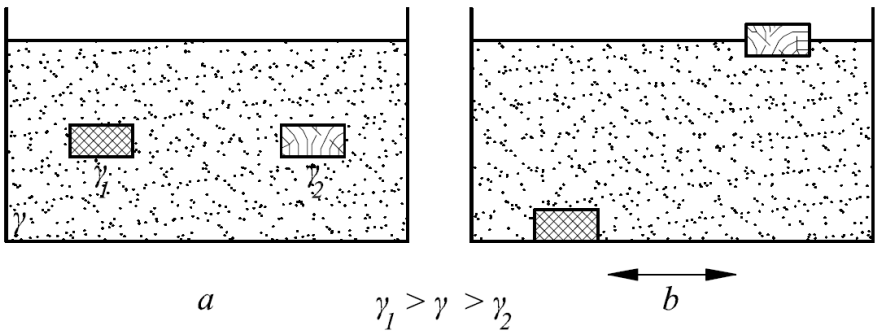

Figure 10. a) state of rest b) state developed as a result of the vibration

As a result of the vibration the components of the granular material, the grains collides into each other, and due to this effect the pressure changes to $h\gamma$ in every direction.

Stresses in the non-cohesive granular materials

We performed the examination of the horizontal plane quadrant cut out by the vertical plane in the proving procedure of the Law III. If this plane inclines towards the material compared to the vertical, – closing an angle β with the horizontal, - and the terrain is horizontal, then, generalizing the former deduction the magnitude of lateral pressure of this granular assembly can be determined in the plane of angle β.

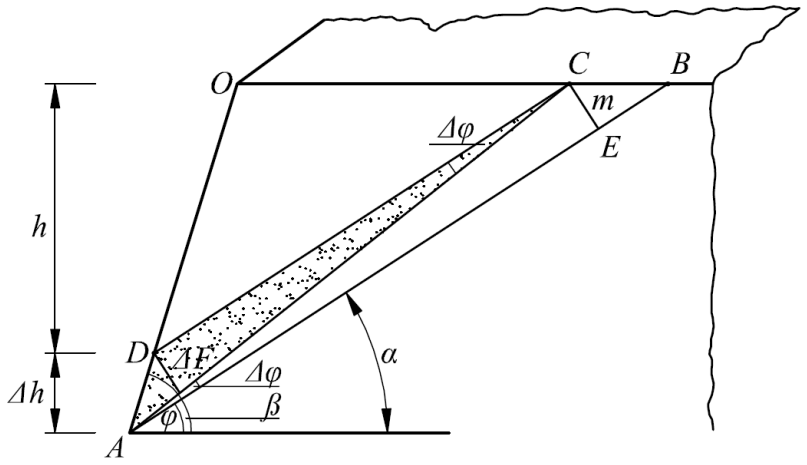

Figure 11. Infinite quadrant of the horizontal terrain confined with an inclined plane

Using the markings of Figure 1, it can be said that the *ADC* granular material weighs on the slope with an inclination angle $\alpha = \varphi + \Delta\varphi$, produced as the result of the Δh

depth increase(as it is marked on Figure 11) with its self-weight (*ΔG*) and with the weight of the material above it (*G*). Line segment *Δh* supports the *ADC* material amount in order to prevent its sliding down. Since *Δh* is very little, therefore, the stress distribution can be considered even in the area, thus the following can be formulated for the slope-direction stress rising there:

$$\sigma_\alpha = \frac{(G + \Delta G)(\sin\alpha - \mu\cos\alpha)}{\Delta F},$$

where the *ΔF* is the projection of the surface segment *Δh* perpendicular to the slope.

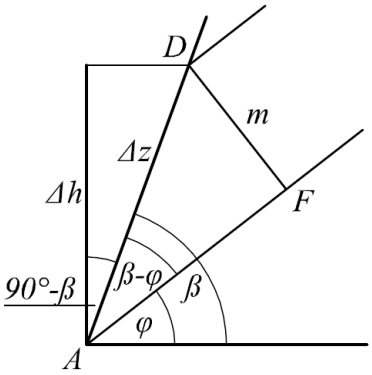

Figure 12. Δh part of Figure 11.

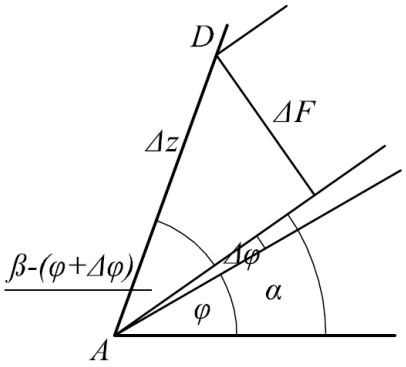

Figure 13. ΔF part of figure 11.

The *G* given in the equation can be expressed for the unit-long space parts *ΔG* and *ΔF* from Figures 11, 12 and13:

$$G = \frac{h^2\gamma}{2}(ctg\,\varphi - ctg\,\beta),$$

and

$$\Delta G = \frac{m}{2}\cdot\frac{h}{\sin\varphi}\cdot\gamma,$$

where *m* can be expressed with the help of Figure 11:

$$m = \Delta z\cdot\sin(\beta-\varphi), \text{ and } \Delta z = \frac{\Delta h}{\cos(90^0-\beta)},$$

thus

$$m = \frac{\Delta h}{\cos(90^0-\beta)}\sin(\beta-\varphi),$$

that is

$$m = \frac{\Delta h}{\sin\beta}\sin(\beta - \varphi),$$

Replacing the value of the *m* into the relation written for the *ΔG*:

$$\Delta G = \frac{h\Delta h\gamma}{2} \cdot \frac{\sin(\beta - \varphi)}{\sin\varphi \cdot \sin\beta}.$$

The value of *ΔF* can be expressed with the help of Figure 13:

$$\Delta F = \Delta z \sin\left[\beta - (\varphi + \Delta\varphi)\right],$$

$$\Delta F = \frac{\Delta h}{\sin\beta}\sin\left[\beta - (\varphi + \Delta\varphi)\right].$$

The equality $\sin\alpha - \mu\cos\alpha = \frac{\sin\Delta\varphi}{\cos\varphi}$ was deduced during the proof of the Law II.

Replacing the value of *G*, *ΔG*, *ΔF* and $\sin\alpha - \mu\cdot\cos\alpha$ into the relation written for the σ_α:

$$\sigma_\alpha = \frac{\frac{h^2\gamma}{2}(ctg\varphi - ctg\beta) + \frac{h\Delta h\gamma}{2}\frac{\sin(\beta-\varphi)}{\sin\varphi\cdot\sin\beta}}{\frac{\Delta h}{\sin\beta}\sin\left[\beta - (\varphi + \Delta\varphi)\right]} \cdot \frac{\sin\Delta\varphi}{\cos\varphi},$$

$$\sigma_\alpha = \frac{h\gamma}{2} \cdot \frac{\sin\Delta\varphi\sin\beta}{\Delta h\cos\varphi} \cdot \frac{h(ctg\varphi - ctg\beta) + \Delta h\frac{\sin(\beta-\varphi)}{\sin\varphi\cdot\sin\beta}}{\sin\left[(\beta-\varphi) - \Delta\varphi\right]},$$

$$\sigma_\alpha = \frac{h\gamma}{2} \cdot \frac{\sin\Delta\varphi}{\Delta h\cos\varphi} \cdot \frac{h(ctg\varphi\cdot\sin\beta - \cos\beta) + \Delta h\frac{\sin\beta\cdot\cos\varphi - \cos\beta\cdot\sin\varphi}{\sin\varphi}}{\sin(\beta-\varphi)\cdot\cos\Delta\varphi - \cos(\beta-\varphi)\cdot\sin\Delta\varphi},$$

$$\sigma_\alpha = \frac{h\gamma}{2} \cdot \frac{1}{\Delta h\cos\varphi} \cdot \frac{h(ctg\varphi\cdot\sin\beta - \cos\beta) + \Delta h(ctg\varphi\cdot\sin\beta - \cos\beta)}{ctg\Delta\varphi\cdot\sin(\beta-\varphi) - \cos(\beta-\varphi)},$$

$$\sigma_\alpha = \frac{h\gamma}{2} \cdot \frac{h + \Delta h}{\Delta h\cos\varphi} \cdot \frac{ctg\varphi\cdot\sin\beta - \cos\beta}{ctg\Delta\varphi\cdot\sin(\beta-\varphi) - \cos(\beta-\varphi)},$$

but $ctg\Delta\varphi$ can be expressed from the triangle *ACE* of Figure 11 by employing the triangle *ADF* of Figure 12:

$$ctg\Delta\varphi = \frac{\overline{AE}}{m} = \frac{\overline{CD} + \overline{AF}}{m},$$

where: $\overline{CD} = \frac{h}{\sin\varphi}$ and $\overline{AF} = \Delta z\cdot\cos(\beta - \varphi)$,

but $\Delta z = \dfrac{\Delta h}{\cos(90^0 - \beta)} = \dfrac{\Delta h}{\sin\beta}$,

therefore $\overline{\Delta F} = \dfrac{\Delta h}{\sin\beta}\cos(\beta - \varphi)$,

so

$$ctg\Delta\varphi = \frac{\dfrac{h}{\sin\varphi} + \dfrac{\Delta h}{\sin\beta}\cos(\beta - \varphi)}{m},$$

since $m = \dfrac{\Delta h}{\sin\beta}\sin(\beta - \varphi)$,

$$ctg\Delta\varphi = \frac{\dfrac{h}{\sin\varphi} + \dfrac{\Delta h}{\sin\beta}\cos(\beta - \varphi)}{\dfrac{\Delta h}{\sin\beta}\sin(\beta - \varphi)},$$

$$ctg\Delta\varphi = \frac{h\sin\beta + \Delta h\sin\varphi\cdot\cos(\beta - \varphi)}{\Delta h\sin\varphi\cdot\sin(\beta - \varphi)},$$

$$ctg\Delta\varphi = \frac{h\sin\beta}{\Delta h\sin\varphi\cdot\sin(\beta - \varphi)} + ctg(\beta - \varphi);$$

replacing the value of $ctg\Delta\varphi$ into the relation of the σ_α:

$$\sigma_\alpha = \frac{h\gamma}{2}\cdot\frac{h + \Delta h}{\Delta h\cos\varphi}\cdot\frac{ctg\varphi\cdot\sin\beta - \cos\beta}{\dfrac{h\sin\beta\cdot\sin(\beta - \varphi)}{\Delta h\sin\varphi\cdot\sin(\beta - \varphi)} + \dfrac{\cos(\beta - \varphi)\cdot\sin(\beta - \varphi)}{\sin(\beta - \varphi)} - \cos(\beta - \varphi)},$$

$$\sigma_\alpha = \frac{h\gamma}{2}\cdot\frac{h + \Delta h}{\Delta h\cos\varphi}\cdot\frac{ctg\varphi\cdot\sin\beta - \cos\beta}{\dfrac{h\sin\beta}{\Delta h\sin\varphi} + \cos(\beta - \varphi) - \cos(\beta - \varphi)},$$

$$\sigma_\alpha = \frac{h\gamma}{2}\cdot\frac{(h + \Delta h)(ctg\varphi\cdot\sin\beta - \cos\beta)\sin\varphi}{h\sin\beta\cdot\cos\varphi},$$

$$\sigma_\alpha = \frac{h + \Delta h}{2}\gamma(1 - ctg\beta\cdot tg\varphi),$$

if Δh is very little, that is $\Delta h \to 0$, then $\alpha \to \varphi$, consequently $\sigma_\alpha \to \sigma_\varphi$, i.e. the direction of the stress closes an angle φ with the horizontal.

Consequently

$$\lim_{\Delta h\to 0}\sigma_\alpha = \frac{h\gamma}{2}(1 - ctg\beta\cdot tg\varphi),$$

that is

$$\boxed{\sigma_{\varphi} = \frac{h\gamma}{2}\left(1 - \frac{tg\varphi}{tg\beta}\right)}.$$

The horizontal component of the σ_{φ} is:

$$\boxed{\sigma_h = \frac{h\gamma}{2}(\cos\varphi - \frac{\sin\varphi}{tg\beta})}.$$

Examining the three special values of the slope angle β of the plane, (which is the angle at which the plane inclines to the horizontal), it can be established that if $\beta = \varphi$, then $\sigma_{\varphi} = 0$, i.e. the non-cohesive granular material will stop in the free slope without support.

If $\beta = 90^0$, then the static pressure acting on this plane is:

$$\sigma_{\varphi} = \frac{h\gamma}{2}, \text{ and } \sigma_h = \frac{h\gamma}{2}\cos\varphi.$$

If $\beta = 45^0 + \frac{\varphi}{2}$, then the static pressure acting on this plane is:

$$\sigma_{\varphi} = \frac{h\gamma}{2} \cdot \frac{1}{1+\sin\varphi}, \text{ and } \sigma_h = \frac{h\gamma}{2} tg\left(45^0 - \frac{\varphi}{2}\right).$$

Active stress state

Development of the active stress state

The small-size horizontal-direction displacement – tilt – of the vertical wall supporting the non-cohesive granular material being in a state of rest causes expansion in the material. The motion of the material follows the displacement of the retaining wall into the horizontal direction loosened up, which appears as a relatively two-direction displacement from a given point of the interior of the material. As a result of the displacement following the expansion, the effect of the shear stresses mobilised by the horizontal stress components of the static pressure ceases (breaks up). The relatively two-direction displacement inside the material terminates the vertical-direction shear stresses in pairs, therefore the vertical stress increases to $h\gamma$. At the same time the material begins to carry out a consolidation motion.

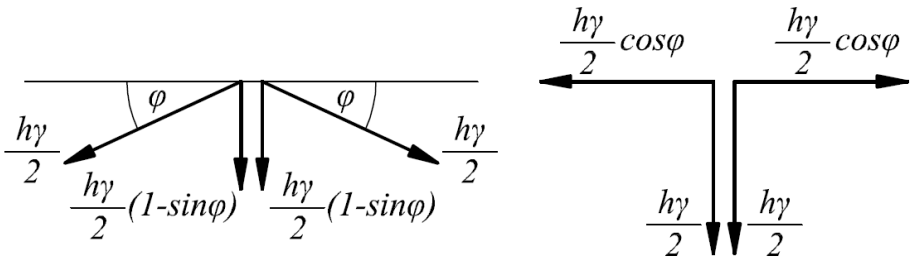

Figure 14. Stress model in quiescent a position

The vertical stress of Figure 7 and 8 (state of rest) can be divided into two stresses of the same size and direction (Fig. 14). The development of the active stress state can be explained in the horizontal-surface non-cohesive granular materials by the change of the so obtained stress model. The shear stresses, which were terminated due to the effect of the expansion, change the stress model of Figure 14 to that of Figure 15.

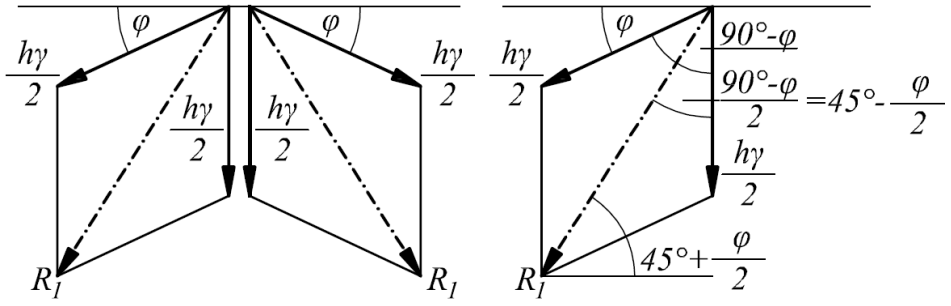

Figure 15. Change of the stress model in an active state

The consolidation motion occurs in the direction of the biggest stresses, i.e. in the direction of the stress resultants. The directions of the resultants of the stress pairs – which can be read from Figure 15 – incline at an angle $45^0 + \frac{\varphi}{2}$ to the horizontal and at an angle $90^0 - \varphi$ to each other. Considering the acting (resultant) stress directions this stress condition consequently, corresponds to the *Rankine* active stress state. Stress R_1 starts the consolidation motion. This motion is reduced by the multiplication product of $tg\varphi$ and stress R_2 - a stress perpendicular to the stress R_1 - , R_1 mobilises shear stress. The magnitude of stress *K* inclining at an angle $45^0 + \frac{\varphi}{2}$ to the horizontal, consequently is

$$K = R_1 - R_2 \cdot tg\varphi.$$

Stress R_1 consists of two stresses. R_1 and R_2 can be expressed from the illustrations of the stress vectors in Figure 16.

Stress R_1 presents itself as the sum of two stresses; the sum of its stress components taken for this direction (R_2) develops the shear stress.

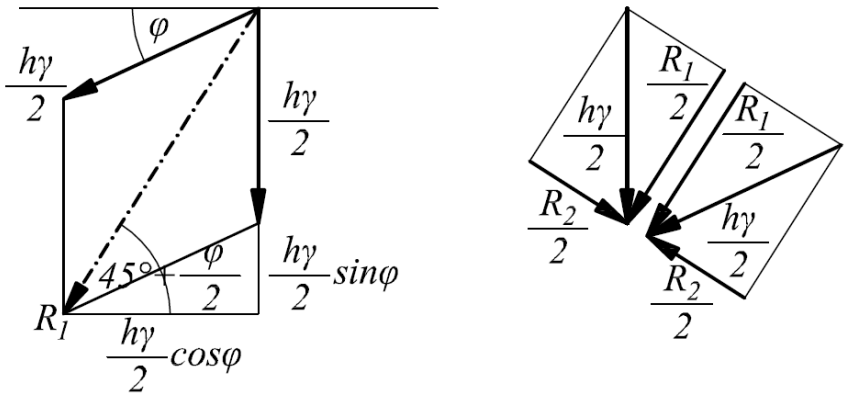

Figure 16. The motion started by the resultant stress mobilises shear tress

$$R_1 = 2\frac{h\gamma}{2}\sin\left(45^0 + \frac{\varphi}{2}\right),$$

and

$$R_2 = 2\frac{h\gamma}{2}\cos\left(45^0 + \frac{\varphi}{2}\right),$$

thus

$$K = h\gamma\sin\left(45^0 + \frac{\varphi}{2}\right) - tg\varphi \cdot h\gamma\cos\left(45^0 + \frac{\varphi}{2}\right).$$

The horizontal component of the resultant stress K:

$$K_h = K\cos\left(45^0 + \frac{\varphi}{2}\right),$$

$$K_h = h\gamma\sin\left(45^0 + \frac{\varphi}{2}\right)\cos\left(45^0 + \frac{\varphi}{2}\right) - h\gamma \cdot tg\varphi \cdot \cos^2\left(45^0 + \frac{\varphi}{2}\right),$$

$$K_h = h\gamma\left[\frac{1}{2}\sin 2\left(45^0 + \frac{\varphi}{2}\right) - tg\varphi \cdot \frac{1}{2}(1 - \sin\varphi)\right],$$

because

$$\cos^2\left(45^0 + \frac{\varphi}{2}\right) = \frac{1}{2}(1 - \sin\varphi),$$

that is

$$\cos^2\left(45^0 + \frac{\varphi}{2}\right) = \left[\frac{\sqrt{2}}{2}\left(\cos\frac{\varphi}{2} - \sin\frac{\varphi}{2}\right)\right]^2,$$

$$\cos^2\left(45^0+\frac{\varphi}{2}\right)=\frac{1}{2}\left[\sqrt{\frac{1+\cos\varphi}{2}}-\sqrt{\frac{1-\cos\varphi}{2}}\right]^2,$$

$$=\frac{1}{2}\left[\frac{1+\cos\varphi}{2}-2\sqrt{\frac{1+\cos\varphi}{2}\cdot\frac{1-\cos\varphi}{2}}+\frac{1-\cos\varphi}{2}\right],$$

$$=\frac{1}{2}\left[1-2\sqrt{\frac{1-\cos^2\varphi}{4}}\right],$$

$$=\frac{1}{2}(1-\sin\varphi).$$

$$K_h=\frac{h\gamma}{2}\left[\cos\varphi-\frac{\sin\varphi}{\cos\varphi}(1-\sin\varphi)\right],$$

$$K_h=\frac{h\gamma}{2}\cdot\frac{\cos^2\varphi-\sin\varphi(1-\sin\varphi)}{\cos\varphi},$$

$$K_h=\frac{h\gamma}{2}\cdot\frac{\cos^2\varphi-\sin\varphi+\sin^2\varphi}{\cos\varphi},$$

$$K_h=\frac{h\gamma}{2}\cdot\frac{1-\sin\varphi}{\cos\varphi},$$

$$\boxed{K_h=\frac{h\gamma}{2}\cdot tg\left(45^0-\frac{\varphi}{2}\right)}.$$

The vertical component of the resultant stress K is K_v.

$$K_v=K\sin\left(45^0+\frac{\varphi}{2}\right),$$

$$K_v=h\gamma\sin^2\left(45^0+\frac{\varphi}{2}\right)-tg\varphi\cdot h\gamma\cdot\sin\left(45^0+\frac{\varphi}{2}\right)\cos\left(45^0+\frac{\varphi}{2}\right),$$

since $\sin^2\left(45^0+\frac{\varphi}{2}\right)=\frac{1}{2}(1+\sin\varphi)$ and $\sin\left(45^0+\frac{\varphi}{2}\right)\cos\left(45^0+\frac{\varphi}{2}\right)=\frac{1}{2}\cos\varphi$,

thus $K_v=\frac{1}{2}h\gamma(1+\sin\varphi-tg\varphi\cdot\cos\varphi)$,

$$K_v=\frac{1}{2}h\gamma\left(1+\sin\varphi-\frac{\sin\varphi}{\cos\varphi}\cos\varphi\right),$$

$$K_v=\frac{h\gamma}{2}.$$

The resultant stress K is

$$K = \sqrt{K_h^2 + K_v^2},$$

$$K = \frac{h\gamma}{2}\sqrt{tg^2\left(45^0 - \frac{\varphi}{2}\right)+1},$$

$$K = \frac{h\gamma}{2}\sqrt{\frac{\sin^2\left(45^0 - \frac{\varphi}{2}\right)}{\cos^2\left(45^0 - \frac{\varphi}{2}\right)} + \frac{\cos^2\left(45^0 - \frac{\varphi}{2}\right)}{\cos^2\left(45^0 - \frac{\varphi}{2}\right)}},$$

$$K = \frac{h\gamma}{2}\sqrt{\frac{\sin^2\left(45^0 - \frac{\varphi}{2}\right) + \cos^2\left(45^0 - \frac{\varphi}{2}\right)}{\cos^2\left(45^0 - \frac{\varphi}{2}\right)}},$$

$$K = \frac{h\gamma}{2}\sqrt{\frac{1}{\cos^2\left(45^0 - \frac{\varphi}{2}\right)}},$$

$$K = \frac{h\gamma}{2}\cdot\frac{1}{\cos\left(45^0 - \frac{\varphi}{2}\right)}.$$

Comparing the value of the K with the value of the σ_φ – which is $\frac{h\gamma}{2}$ - it is conceivable that the K is bigger. Therefore, in case of expansion, or in case of a more significant displacement of the wall supporting the granular material the motion direction of the material inclines at an angle of $45^0 + \frac{\varphi}{2}$ to the horizontal.

Due to the expansion the stress starting the motion can be illustrated according to Figure 17.

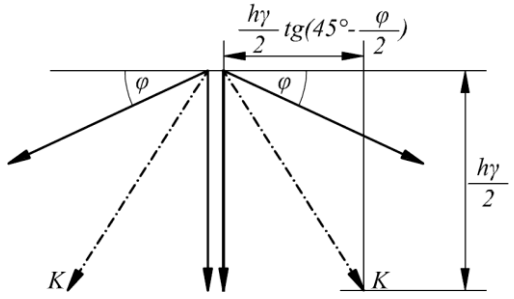

Figure 17. Motion starting stress in an active state

The motion is realised towards the direction of the resultants of the stresses, consequently, in the direction inclining at an angle of $45^0 + \frac{\varphi}{2}$ to the horizontal. The material moves with its whole material amount, i.e. infinitely many slip planes inclining at an angle of $45^0 + \frac{\varphi}{2}$ to the horizontal are developed.

The horizontal component of the resultant stress K is σ_x, i.e.

$$\sigma_x = K \cdot \cos\left(45^0 + \frac{\varphi}{2}\right) = K \cdot \sin\left(45^0 - \frac{\varphi}{2}\right),$$

$$\sigma_x = \frac{h\gamma}{2} \cdot \frac{\sin\left(45^0 - \frac{\varphi}{2}\right)}{\cos\left(45^0 - \frac{\varphi}{2}\right)},$$

$$\sigma_x = \frac{h\gamma}{2} \cdot tg\left(45^0 - \frac{\varphi}{2}\right).$$

Pressure acting on the vertical retaining wall

If the horizontal-terrain non-cohesive granular material is supported by a real, frictional, vertical wall, and an expansion occurs in the material due to its displacement, then the stresses acting on the wall can be determined with the knowledge of the angle (δ) of the friction rising on the wall:

A stress with a magnitude of σ_δ, inclining at an angle δ to the horizontal acts on the wall. The $\sin\delta$-fold amount of this stress reduces the vertical stress $\frac{h\gamma}{2}$ to $\frac{h\gamma}{2} - \sigma_\delta \sin\delta$. The horizontal stress component: $\sigma_\delta \cos\delta$ is in direct proportion to

the vertical stress, just as the ratio of the vertical $\frac{h\gamma}{2}$ and the horizontal $\frac{h\gamma}{2}\cos\varphi$ stress components is constant in the stress model acting inside the material. Consequently the proportion can be written:

$$\frac{\frac{h\gamma}{2}}{\frac{h\gamma}{2}\cdot\cos\varphi}=\frac{\frac{h\gamma}{2}-\sigma_\delta\sin\delta}{\sigma_\delta\cos\delta}.$$

The σ_δ can be expressed:

$$\frac{h\gamma}{2}\sigma_\delta\cdot\cos\delta=\frac{h\gamma}{2}\left(\frac{h\gamma}{2}\cos\varphi-\sigma_\delta\cdot\sin\delta\cdot\cos\varphi\right),$$

$$\sigma_\delta\cdot\cos\delta+\sigma_\delta\cdot\sin\delta\cdot\cos\varphi=\frac{h\gamma}{2}\cos\varphi,$$

$$\sigma_\delta(\cos\delta+\sin\delta\cdot\cos\varphi)=\frac{h\gamma}{2}\cos\varphi,$$

$$\sigma_\delta=\frac{h\gamma}{2}\cdot\frac{\cos\varphi}{\cos\delta+\sin\delta\cdot\cos\varphi}.$$

The horizontal component of the σ_δ is σ_h:

$$\sigma_h=\sigma_\delta\cos\delta,$$

$$\sigma_h=\frac{h\gamma}{2}\cdot\frac{\cos\varphi\cdot\cos\delta}{\cos\delta+\sin\delta\cdot\cos\varphi},$$

$$\boxed{\sigma_h=\frac{h\gamma}{2}\cdot\frac{\cos\varphi}{1+tg\delta\cdot\cos\varphi}}.$$

The obtained result shows, that if no friction were developed on the retaining wall, then the static pressure would act on it; or looking at it from the other way round: no friction rises on the retaining wall when static pressure develops. This is proved by the evidence of the model experiments.

If the friction rising on the retaining wall were equal to the friction rising inside the granular material, i.e. $\delta=\varphi$, then active pressure would act on the retaining wall, which pressure also prevails inside the material in the active stress state. If δ does not reach the value of the φ, then an intermediate stage – between the static pressure and active pressure – emerges near the retaining wall.

In the past several people performed experimental measurements with dry sand – a non-cohesive granular material –. for the determination of the lateral pressure. Taking accuracy and model size into consideration the experiments started by Terzaghi in 1929 rose above the other researches. In his experiment the retaining wall was a 2.1-metre-high and 4.2-metre-long rigid reinforced concrete structure. The volume of the sandbox was 37 m^3 and the displacement of the wall was measured with an accuracy of 0.0025 mm. The results of the experiment can be summed up as follows:

While the retaining wall was motionless, a horizontal, static pressure with the magnitude of $E_0 = 0.42\frac{h^2\gamma}{2}$ acted on it. At the slight displacement of the wall the lateral pressure decreased, then due to further displacement, tilt of the retaining wall, the horizontal component of the lateral pressure became constant near the value of $0.29\frac{h^2\gamma}{2}$, while the tangent of the friction developed on the retaining wall moved near the value $tg\delta = 0.54$. Due to the expansion that occurred in the sand, and as a result of the loosening the surface sank near the displaced wall.

The measured values correspond well to the result obtained by means of the previously deduced theoretic formulas:

- the static pressure coefficient was $\lambda = 0.42$,

$$\lambda = \frac{\cos\varphi}{2},$$

$$\cos\varphi = 2 \cdot 0.42,$$

$\varphi = 32.85^0$, which is a value characteristic of the dry sand.

- the horizontal stress component of the pressure acting on the frictional retaining wall is:

$$\sigma_h = \frac{h\gamma}{2} \cdot \frac{\cos\varphi}{1 + tg\delta \cdot \cos\varphi},$$

the measured value $\cos\varphi = 0.84$ and $tg\delta = 0.54$,

$$\sigma_h = \frac{h\gamma}{2} \cdot \frac{0.84}{1 + 0.54 \cdot 0.84},$$

$$\sigma_h = h\gamma \cdot 0.2889,$$

i.e. it is remarkably consistent with the expected measured value of ca. 0.2889≈0.29.

Arch formation in granular materials

The phenomenon of the arch formation is one of the basic questions of the mechanics of the granular materials. The theoretical clarification of arch formation provides solution to such direct practical problems, as the bulk storage of granular materials in silos or their safe discharge. In the hoppers of the silos the material often coagulates, or an arch is formed, which impedes the gravitational discharge.

Condition of arch formation

In each case it is always the displacement of a part of the material, which generates arch formation. This motion can originate from consolidation, compaction or, for example, from the material motion that follows the opening of the gate located on the bottom of the hopper. Due to the displacement, the stresses in the material are rearranged in a way that the retaining part of the material that remains in place takes over also part of the stresses of the moving material part. If the stresses, which rose this way are big enough and their direction is adequate, an arch will be formed in the material, which will prevent any further displacement. The arch-forming effect of the displacement prevails, when the material must undergo specific deformation during the displacement, i.e. it must pass through for example a narrowing cross-section.

On the basis of the aforementioned considerations, if we want to follow the process of arch formation, an infinitely long symmetric trough with narrowing cross-section, filled with non-cohesive granular material (Fig. 18) can be chosen as the starting point of the examination.

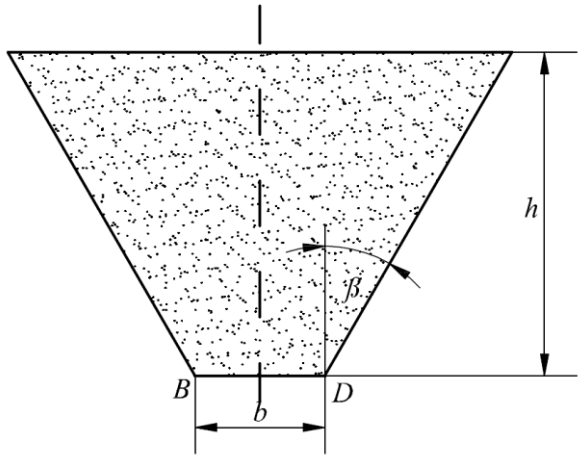

Figure 18. Dimensions of the trough

Let us assume, that the volume weight of the material (γ) does not change as a function of the depth and the material does not compress after the filling. A movable bottom-plate closes the b-wide lower opening of the trough, which has a flat and rigid side wall inclining outwards with an angle β to the vertical. The assumption of an infinite length makes the planar examination of the case possible. After the removal of the bottom-plate of the trough the material moves off – it wants to flow out – and undergoes specific deformation as a result of the narrowing cross-section; consequently the model ensures the conditions of arch formation as described before.

If the granular material is at a quiescent state and the side walls are rigid, then static pressure develops inside the material; consequently the pressure is $h\gamma$ in the vertical and $\lambda h\gamma$ in the horizontal direction, where λ is the quotient of the vertical and horizontal pressure i.e. it is the coefficient of the static pressure.

The stresses acting on the side wall inclining outwards at an angle β to the vertical, and respectively the resultant force of the stresses (E) can be determined according to magnitude and direction on the basis of Figure 19:

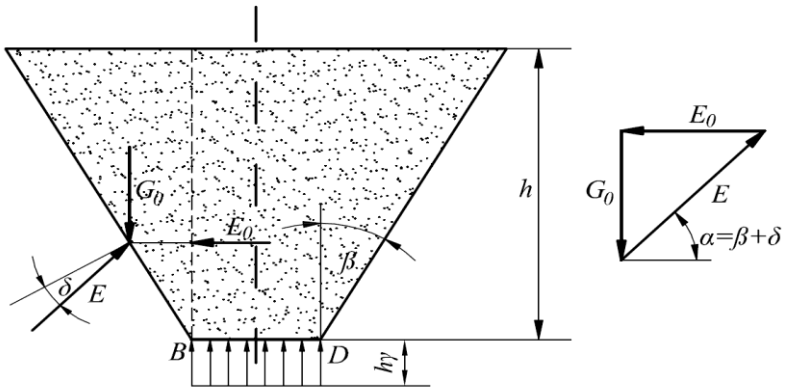

Figure 19. Force equilibrium of the trough with a closed bottom plate, filled with granular material

G_0 is the weight of the material part between the vertical plane and the side wall, which is inclining outwards at an angle β:

$$G_0 = \frac{h^2\gamma}{2} tg\beta,$$

E_0 is the resultant force of the horizontal static pressure:

$$E_0 = \lambda \frac{h^2\gamma}{2}.$$

The resultant force from the vector triangle is:

$$E = \frac{h^2\gamma}{2}\sqrt{\lambda^2 + tg^2\beta}.$$

For the inclination angle of the resultant force, inclined to the horizontal plane it can be written:

$$tg\alpha = \frac{G_0}{E_0},$$

that is

$$tg\alpha = \frac{tg\beta}{\lambda}.$$

If the side wall can take up the α-direction force and the stresses due to the lateral wall friction, then only vertical stresses with a magnitude of $h\gamma$ act on the bottom

plate. This is only true, if $\alpha \leq \beta + \delta,$ where the δ is the angle of the friction on the side wall, rising between the wall and the material.

After removing the horizontal plate closing the discharge opening of the trough, shear planes form inside the material, due to the fact that the material can pass through the narrowing cross-section only by shear. If $\alpha \leq \beta + \delta$, i.e. only vertical stresses acted previously on the horizontal plate, then the plane of the shear will be vertical. Since the material is sheared on that surface, to which the smallest force is needed. The force necessary for shearing the non-cohesive granular material is expressed by the relation, $F = A\sigma_n tg\varphi$, using the *Coulomb's* equation, where

A —is the sheared surface,

σ_n — is the perpendicular stress acting on the sheared surface,

φ — is the friction angle of the material.

The smallest shear force is necessary for the shearing of the vertical plane, since the sheared surface is the smallest here and it is also the plane where the horizontal stresses are the smallest. (The horizontal stresses are always smaller than the vertical or intermediate-direction stresses) Consequently, the plane of the shear is vertical.

From both of the points *B* and *D* of the trough a vertical shear plane is formed, if the vertical-direction force rising from the weight of the material part located above the opening *b* is equal with the shear force demand of the two planes:

$$b \cdot h \cdot \gamma = 2\lambda \frac{h^2 \gamma}{2} tg\varphi,$$

that is

$$b = h\lambda \cdot tg\varphi .$$

If the size of *b* is bigger than this value, then the material with a $\lambda h \cdot tg\varphi$ width is torn off in one part and takes with itself – under the effect of the acting shear stresses - the other material parts as far as the total opening *b* of the trough.

If $b \leq \lambda h \cdot tg\varphi$, then only two vertical-direction shear surfaces develops after the removal of the plate closing the discharge opening of the trough. At this time shear stresses arise inside the material on the shear plane, which are produced by the vertical weight force $b \cdot h \cdot \gamma$. The material part, which is located between the shear

plane and the side wall of the trough takes up the vertical shear forces *F*, and transfers them to the side walls. The side wall can only take up this vertical-direction plus force entirely if the resultant force (E_B) does not exceeds the angle of the friction arising on the side wall.

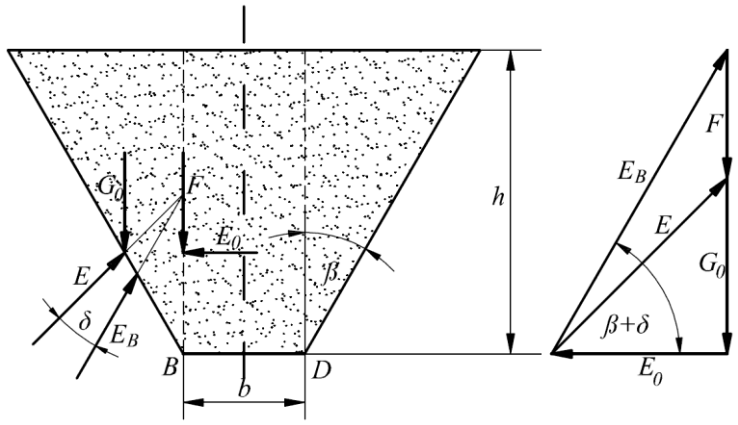

Figure 20. Force equilibrium after the removal of the bottom plate of the trough

It is well discernible on the vector polygon of Figure 20 that the resultant force E_B does not exceed the friction angle δ, if the inclination angle of the side wall and the friction arising there is big enough, i.e. $\alpha \le \beta + \delta$. From the vector diagram the following can be formulated for the limit case

$$tg(\beta+\delta) = \frac{F+G_0}{E_0}.$$

The shear force *F* is the half of the material weight above the opening, since it is divided into two shear planes, consequently

$$F = \frac{bh\gamma}{2},$$

furthermore $$G_0 = \frac{h^2\gamma}{2} tg\beta \text{ an } E_0 = \lambda \frac{h^2\gamma}{2}.$$

Substituting the values of the *F*, G_0 an E_0 into the relation written for the *tg (β+δ)* we get:

$$tg(\beta+\delta) = \frac{\frac{bh\gamma}{2} + \frac{h^2\gamma}{2} tg\beta}{\lambda \frac{h^2\gamma}{2}},$$

simplified: $$tg(\beta+\delta)=\frac{b+h\cdot tg\beta}{\lambda h}$$

consequently, if $b \le \lambda h \cdot tg\varphi$, then starting from the lower opening of the trough, individual shear planes are formed and the side wall can take up the weight of the material part located between them by the rearrangement of the shear stresses, if

$$tg(\beta+\delta) \ge \frac{b+h\cdot tg\beta}{\lambda h}.$$

In this case the material cannot flow out and an arch is formed above the opening. From the relation $b \le \lambda h \cdot tg\varphi$ and the relation obtained for the $tg(\beta+\delta)$ the relationship $\frac{b}{h}$ can be expressed:

$$\frac{b}{h} \le \lambda \cdot tg\varphi,$$

$$\frac{b}{h} \le \lambda \cdot tg(\beta+\delta) - tg\beta.$$

These two equalities and inequalities formulate the condition of the formation of the arch in the non-cohesive granular material.

According to the solution of the arch formation, calculated with the help of the resultant forces, the shear force *F* diverts the fulcrum of the resultant force *E* of the quiescent state towards the lower opening of the trough. The intersection point of the line of action of the forces *E* and *F* determines the position of E_B. The deviation is in direct ratio with the increase of the angle β. This deviation can be left out of consideration in case of the practical calculations. Since, in the event of a significant increase of the angle β the arch already rests directly on the material and not on the side wall (see later).

Character of the discharge

The character of the discharge of the granular material flowing out of the trough can be interpreted with the previously deduced arch conditions in cases, when any one of the conditions is not fulfilled.

a) If $\alpha \rangle \beta + \delta$, i.e. $\frac{b}{h} \rangle \lambda \cdot tg(\beta + \delta) - tg\beta$, then the side wall cannot take entirely up the resultant force, which changed due to the rearrangement of the shear stresses. The free component of the resultant force *E,* parallel with the side wall, sets off the slide of the material along the side wall. The material part located between the shear plane and the side wall also moves off and mass flow occurs (Figure 21/a).

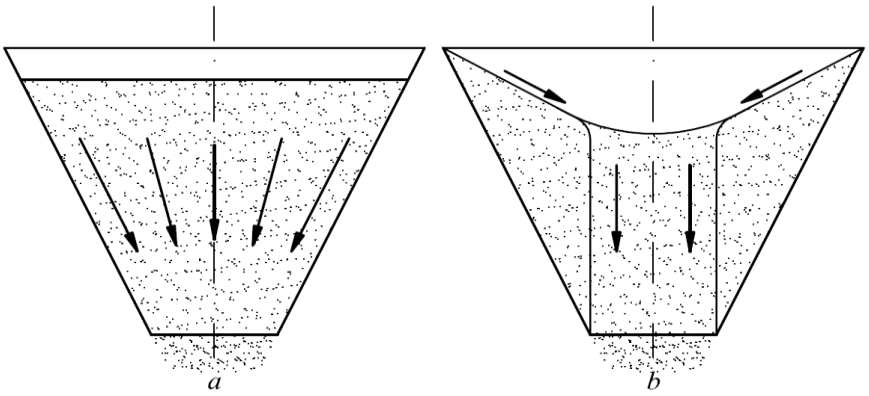

Figure 21. Typical discharges: a) mass flow; b) tunnel flow

b) If $\alpha \langle \beta + \delta$, i.e. $\frac{b}{h} \langle \lambda \cdot tg(\beta + \delta) - tg\beta$, but $b \rangle \lambda h \cdot tg\varphi$ and $\frac{b}{h} \rangle \lambda \cdot tg\varphi$, then even though the side wall can take up the resultant force, but the weight force of the material located above the opening is bigger than the shear force preventing the break away; therefore, the material with a width of *b* flows out vertically, while the material part next to it – the part between the vertical shear plane and the side wall - remains in its place, and flows from above to the vertically moving material part afterwards. Tunnel flow develops (Figure 21/b).

It is easy to see that the character of the discharge is determined not only by the inclination angle and wall friction of the trough, but it is also influenced by the shear resistance, friction angle and the pressure conditions of the material. It can be observed in silos, that certain granular materials are discharged firstly by mass flow, then later by tunnel flow, proving that the pressure conditions dominating in the hopper also influence – though to a smaller extent than the inclination angle and friction of the hopper – the character of the discharge. In the course of our experiments performed with wheat and sand with the application of hoppers with

different inclination angles , it could be observed (when the experiment was carried out in the same hopper and with the same material) that at first mass flow occurred, but when the discharge was continued, the phenomenon of tunnel flow appeared. The change of the character of the material discharge occurred at the pre-calculated height value.

Mechanism of the arch formation

Consequently, the conditions of the arch formation are, that the weight force of the material above the lower opening of the trough should be smaller than then the sum of the shear forces arising on the shear planes, and that due to their inclination angle and wall friction, the side walls should be able to take up the forces acting on the them.

The shear stresses developed after the removal of the plate closing the lower opening of the trough are transferred onto the side wall and summed up with the stresses acting there. These resultant stresses form the arch. The arch surface is formed as a result of a second stress rearrangement.

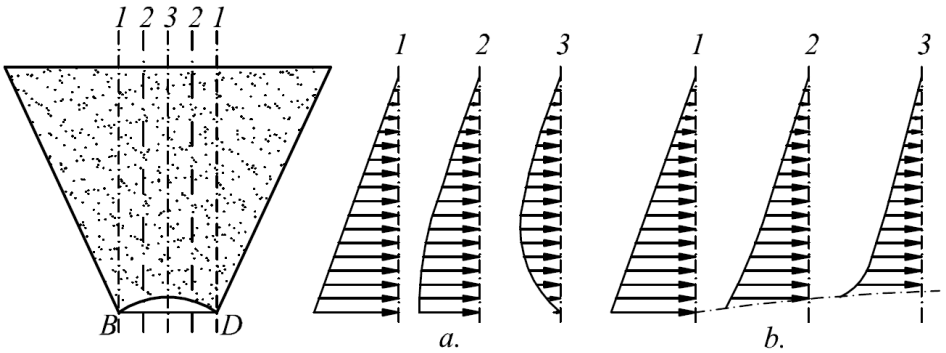

Figure 22. The arch is formed as a result of stress rearrangement

Between the edges *B* and *D* of the trough the distribution of the horizontal components of the resultant stresses is as shown in Figure 22/a. At the places where the horizontal components of the compressive stresses prove to be too small to

support the material against the gravitation – its shear resistance is smaller than its weight force arising from the gravitation – there the dropping of granules. Due to the bleed the stresses rearrange, presumably according to Figure 22/b, in order to provide enough compressive stress for the support of the material. The dropping of granules ceases when identical horizontal stress components – of critical value in terms of the dropping of granules on each point of the arch surface. The fact, that on each point of the arch, the same-value horizontal stress components must act, makes the determination of the equation describing the geometric shape of the arch possible.

Geometric equation of the arch

It is known, if for the support of an evenly distributed load such quadratic parabola is used, in whose end-point only tangential stress develops, then in each point of the parabola only a stress with a parabola-direction, and equal-size horizontal component arises. Such a parabola is loaded by no bending moment, which condition is of vital importance. The bending moments would produce tensile and compressive stresses, which a solid body can withstand, but the non-cohesive granular material is not capable of bearing tensile stresses.

In the points *B* and *D* of the trough an equal-size stress acts in the $\beta+\delta$ –direction, while above the arch there is an almost evenly distributed load. The direction $\beta+\delta$ and the opening width *b* definitely determine the parabola. The maximum rise of the parabola that has the aforementioned characteristics is:

$$f = \frac{b}{4} tg(\beta + \delta).$$

With the coordinate axis *y* placed in the symmetry plane of the opening of the trough, and the axis *x* leading through the points *B* and *D* (Fig. 23) the cuspidal point of the parabola intersects the axis *y* at the height of *C*.

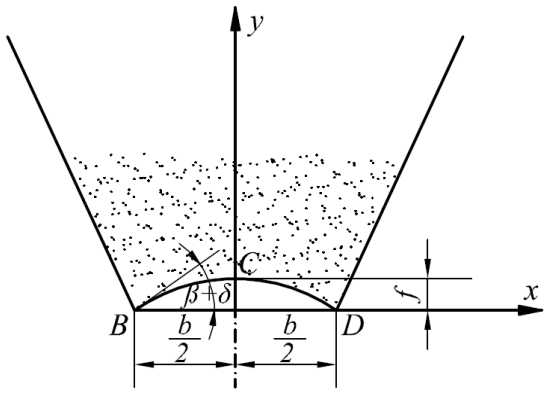

Figure 23. Parabola of the arch

The general form of the equation of the quadratic parabola symmetrical to the axis *y* and running downwards is:

$$y = -Ax^2 + C,$$

since $f=C$, so $C = \frac{b}{4} tg(\beta + \delta)$.

The first differential coefficient of the equation of the parabola at the place of $x = -\frac{b}{2}$ is $y' = tg(\beta + \delta)$, consequently $y = -Ax^2 + C$, $y' = -2Ax$ and

$$tg(\beta + \delta) = 2A\frac{b}{2}.$$

A can be expressed: $A = \frac{1}{b} tg(\beta + \delta)$

Substituting the values of *A* and *C* into the general equation of the parabola:

$$y = -\frac{x^2}{b} tg(\beta + \delta) + \frac{b}{4} tg(\beta + \delta),$$

$$y = \left(\frac{b}{4} - \frac{x^2}{b}\right) tg(\beta + \delta)$$

we get the geometric equation of the arch. From the equation formulating the arch condition the $tg(\beta + \delta)$ can be substituted:

$$y = \left(\frac{b}{4} - \frac{x^2}{b}\right) \frac{b + h \cdot tg\beta}{\lambda h}.$$

In some cases the arch is lower than the form given in the above equation. It occurs when the inclination angle of the trough is big. In this case the arch is supported by that plane of the material, which inclines at an angle ε to the vertical, and $\varepsilon<\beta$. In the material the angle of the friction is φ, therefore, $\varepsilon+\varphi$ substitutes the values of $\beta+\delta$ in the equation that formulates the arch condition and describes the geometric form:

$$\frac{b}{h} \le \lambda \cdot tg(\varepsilon+\varphi) - tg\varepsilon,$$

$$y = \left(\frac{b}{4} - \frac{x^2}{b}\right) tg(\varepsilon+\varphi).$$

The arch leans directly on the material in the case, when $\varepsilon+\varphi$ is smaller than $\beta+\delta$. If from the two arch conditions the equation $\lambda \cdot tg(\beta+\delta) - tg\beta$ restricts the ratio $\frac{b}{h}$, the limit case can be achieved at the identical ratio of $\frac{b}{h}$

$$\lambda \cdot tg(\beta+\delta) - tg\beta = \lambda \cdot tg(\varepsilon+\varphi) - tg\varepsilon.$$

The equation formulated for the limit case gives a solution for the ε only in case of certain $\frac{tg\delta}{tg\varphi}$ values, because it is a quadratic equation and its discriminant can be negative depending on the ratio of δ and φ. If the discriminant is negative, then the arch will continue to lean on the side wall of the trough. If the discriminant is positive, then the equation

$$y = \left(\frac{b}{4} - \frac{x^2}{b}\right) tg(\varepsilon+\varphi)$$

determines the geometric form of the arch.

If from the arch conditions $\lambda \cdot tg\varphi$ restricts the ratio $\frac{b}{h}$, then the angle ε can be calculated from the following relation:

$$\lambda \cdot tg\varphi = \lambda \cdot tg(\varepsilon+\varphi) - tg\varepsilon.$$

Principle of the hopper design

The relations formulating the condition of arch formation in granular media makes the design of such hoppers possible, from which the gravitational discharge of the material can be ensured and which takes up the smallest possible space.

If none of the arch condition is fulfilled, then the gravitational flow is ensured. If

$$\frac{b}{h} \rangle \lambda \cdot tg\varphi ,$$

but

$$\frac{b}{h} \leq \lambda \cdot tg(\beta + \delta) - tg\beta ,$$

then the gravitation discharge takes place in the form of a tunnel flow. If, however,

$$\frac{b}{h} \rangle \lambda \cdot tg(\beta + \delta) - tg\beta ,$$

then the discharge is of mass flow type.

At the design of the hoppers, the goal is, in general, to ensure the mass flow with the smallest discharge opening, in a way that the vertical dimension of the hopper should be the smallest one possible. The principal procedure of the design for a hopper with circular cross-section is as follows.

In the case of hoppers with circular cross-section, instead of a width *b* opening a radius *r* discharge opening must be used, so instead of the equation

$$b \cdot h \cdot \gamma = 2 \cdot \lambda \frac{h^2 \gamma}{2} tg\varphi$$

evidently

$$r^2 \cdot \pi \cdot h \cdot \gamma = 2 \cdot r \cdot \pi \cdot \lambda \frac{h^2 \gamma}{2} tg\varphi ,$$

is written, from which

$$\frac{r}{h} = \lambda \cdot tg\varphi .$$

Before designing the hopper the internal friction angle of the granular material, the friction angle developing on the surface of the hopper and the volume weight must be determined. The friction angles can be determined by shear experiments. The normal loads applied to the material, which was filled in the shear box, must correspond to the expected pressure values in the hopper. For the measurement of the friction angle δ it is advisable to make a packing plate of the material of the hopper for the shear box. The granular material is filled onto the packing plate placed in the shear plane of the shear box, and the angle of the friction is determined by shear experiments. If the material stays in the hopper for a longer period, then the required rheological measurements must also be performed: the shearing is carried out by changing the time of the normal loads acting on the sample. From the tendency of the curves of the material properties drawn in the logarithm of the time the expectable values of the material characteristics during a longer storage period can be concluded. If the granular material is also cohesive, or becomes cohesive in the course of a longer storage, then for the given normal stress value of the shear, the inclination angle to the horizontal axis of the straight-line drawn from the origin, can be taken into account (see later), as the angle of the internal shear resistance (effective friction angle).

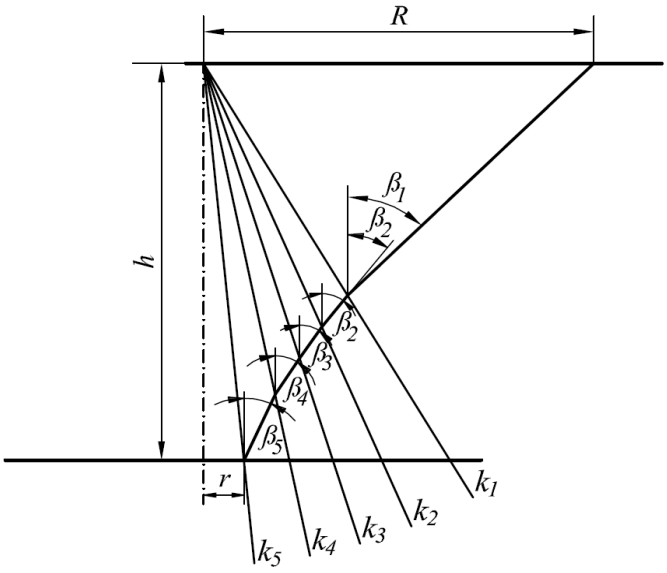

Figure 24. Hopper-design construction

The principal procedure of the hopper design is as follows:

1. Let us determine the value of the $k_1 = \frac{r}{h}$ with the help of the $\lambda \cdot tg\varphi$, which with the substitution of $\lambda = \frac{\cos\varphi}{2}$ is: $k_1 = \frac{r}{h} = \frac{\sin\varphi}{2}$;

2. Let us set up the symmetry axis of the hopper according to Figure 24 and construct straight lines with different $\frac{r}{h}$ ratios;

3. Let us calculate the hopper inclination angle β_1 belonging to the straight line k_1 from the relation $k = \lambda \cdot tg(\beta + \delta) - tg\beta$:

$$\beta = arc \cdot tg \frac{1 - \lambda - k \cdot tg\delta \pm \sqrt{(1 - \lambda - k \cdot tg\delta)^2 - 4\lambda \cdot tg^2\delta + 4k \cdot tg\delta}}{2 \cdot tg\delta};$$

4. Let us draw angle β_1 to the given point of the straight line k_1. (On the upper part of the hopper the mass flow can be ensured by using the hopper inclination angle β_1, by using an angle that is steeper than that.);

5. Let us calculate the value of angle β_2 for a ratio k_2, which is smaller than the critical value k_1;

6. Let us construct angle β_2 on the intersection point obtained on the straight line k_1 and draw its leg as far as the ratio line k_2, then draw the angle β_3 calculated on the basis of the k_3 on the straight line k_2, then continuing the construction and calculation we get a hopper with a curve-constituent approached with individual line segments;

7. By determining the proportion for the given discharge-opening dimension, or for the upper diameter of the hopper, we obtain a dimension-correct hopper shape is obtained, from which the chosen dimensions can be read.

Consequently, the hopper profile ensuring a favourable discharge is a curve.

If technological difficulties justify the construction of a hopper with a straight constituent, then the inclination angle calculated in the dimension of the discharge opening is the decisive factor. If we disregard the mass flow, the only requirement is, that an angle steeper than the natural angle of repose must be chosen instead of the ratio k_1, the inclination angle of the hopper is indifferent. The great advantage of the hopper with curve constituents is, that its build-in space demand is the smallest possible, and it can be inserted as a packing into the existing hoppers, by which the discharge difficulties can be efficiently improved.

The flow-improving advantages of the hyperbolic hoppers with curve constituents are known, which are also proved experimentally by the hoppers designed on the basis of the present theory.

Experimental results

After the elaboration of the theory we carried out measurements with experimental tanks and hopper designed for the given material to be stored. There was a 2 metres high and 1 metre diameter material column above the hopper designed for the material characteristics and friction parameters of the corn-grits. At the straight conical hopper with an inclination angle β=30º an arch was formed as far as the hopper opening with a diameter of 150 mm, which impeded the gravitational discharge. At the same tank but with a hopper with curve-constituents, and with an opening diameter of 100 mm and with the construction of a shorter hopper obtained a safe discharge (Figure 25).

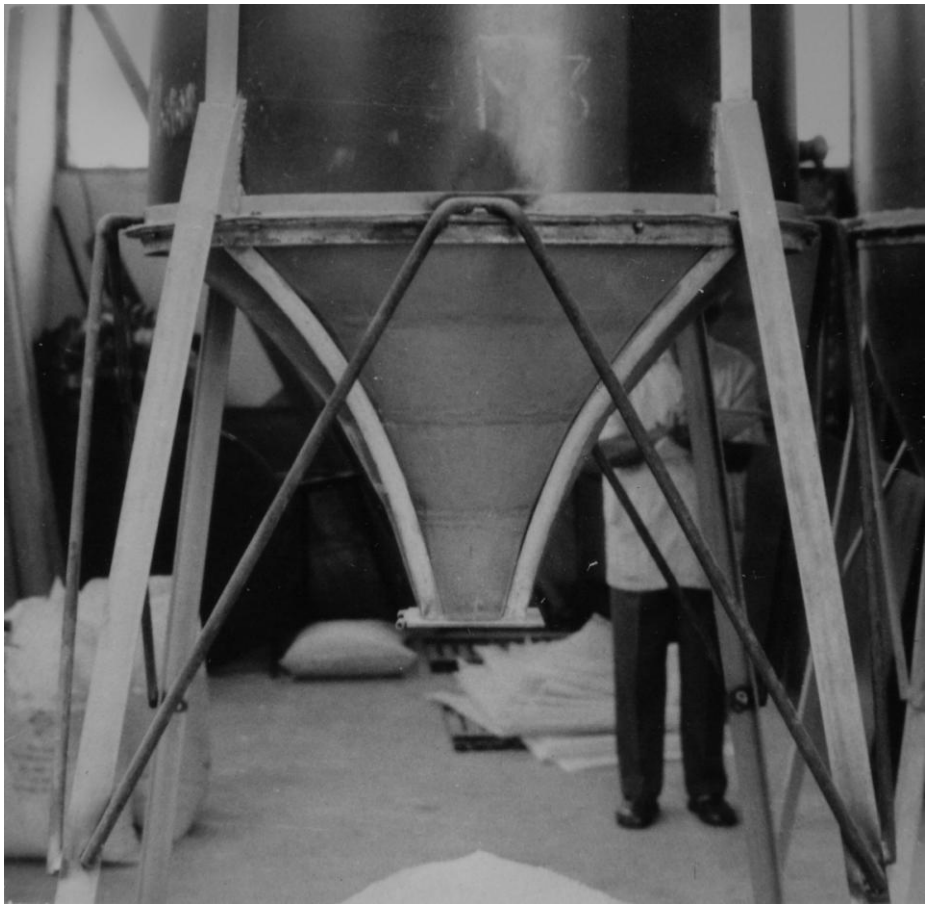

Figure 25. Curve-component hopper

The experimental measurements proved our theoretical calculations not only for corn grits, but also for wetted sand – as a model material – the calculations were furthermore verified with experiments for fertilisers and mixed feeds, for extracted soya grits, feed lime and alfalfa flour.

Stresses in cohesive granular materials

Granular materials generally exhibit, smaller or bigger cohesion depending the on their moisture content. Concerning their mechanical behaviour, the cohesive granular materials show a considerable difference from the non-cohesive granular materials, which justifies their separate treatment.

A cohesive granular material is the conglomeration of large number of solid bodies, which are in constant contact with each other, where the cohesion force between the grains – as the constituting elements of the assembly – is smaller than the cohesive force of the individual grains. Coulomb's friction law pertains to the material and the individual grains keep their shape in spite of forces acting on them.

Lateral Pressure

According to the Coulomb's friction law the shear resistance of the cohesive granular materials can be described by means of the following relation

$$\tau = \sigma_n \cdot tg\varphi + c$$

where:

τ = shear resistance of the material;

σ_n = normal stress acting on the sheared surface;

φ = friction angle of the material;

c = cohesional coefficient.

The shear resistance consists of two parts, the friction (which depends on the pressure acting perpendicularly to the sheared surface) and the cohesion (which is independent of the normal stress).

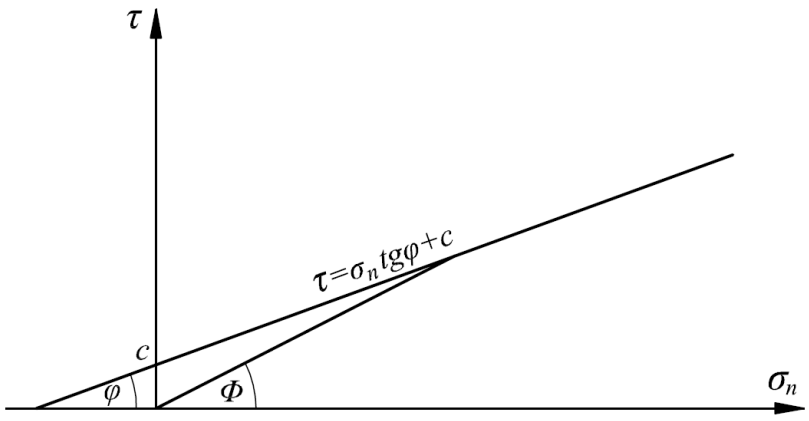

Figure 26. Direct relation of the slip limit angle Φ and the Coulomb's straight-line

The relation $\tau - \sigma_n$ is linear (Figure 26); consequently, it can be represented a straight line, the so called Coulomb's straight-line. The points lying on the straight-line represent the slip limit state, i.e. boundary-equilibrium state. Inside the cohesive granular material, which is in a state of rest, a limit angle belongs to each depth, i.e. to each vertical-direction, $h\gamma$-size stress value, rising from the self-weight, where a slip boundary state can be found. This inclination angle to the horizontal is: Φ, which is the inclinational angle of the straight line linking a given point of the Coulomb's straight-line and the origin, to the horizontal axis (Figure 26). The angle Φ changes depending on the normal stress, i.e. normal stress produced by the self-weight inside the cohesive granular material in a state of rest. Consequently, angle Φ depends also on the depth. On the basis of Figure 26 the following can be formulated for angle Φ:

$$tg\Phi = \frac{\tau}{\sigma_n} \ ,$$

since $$\tau = \sigma_n \cdot tg\varphi + c \ ,$$

and $$\sigma_n = h\gamma \cdot \cos\Phi ,$$

so $$tg\Phi = tg\varphi + \frac{c}{h\gamma \cdot \cos\Phi} .$$

Consequently, the angle Φ depends on the friction angle, the cohesional coefficient, as well as on the product of the depth and volume weight, where the relation is no longer linear. Inside the cohesive material, consequently the surface belonging to the slip boundary state is a curve, the angular coefficient of whose tangent is tg Φ. As a matter of fact angle Φ is nothing else but the angle of the shear resistance, similarly to the friction angle used for the characterisation of the non-cohesive granular material. The physical content of the angle Φ is identical to that of the angle φ of the non-cohesive granular materials. (Angle Φ, which changes as a function of the depth, declines into constant φ in the case of c=0.)

Considering the angle Φ into consideration, the laws II and III concerning the non-cohesive granular materials can be applied to the cohesive granular materials, as well:

II. In the cohesive granular materials at a quiescent state the stresses developed by the vertical-direction compressive stresses act downwards in the zone $\pm 90^0 - \varphi$ measured from the vertical direction (where the Φ is the angle of the internal shear resistance of the material).

III. The static pressure value of the cohesive granular material, rising from the self-weight, is the half of the product of the depth and the volume weight $\left(\frac{h\gamma}{2}\right)$, its direction deviates downwards from the horizontal with the angle of the internal shear resistance of the material. The horizontal component of the static pressure:

$$\boxed{\sigma_x = \frac{h\gamma}{2}\cos\Phi.}$$

The application of the static pressure of the non-cohesive granular material for the cohesive granular material becomes feasible due to the fact, that in granular materials the ratio between the vertical stress rising from the self-weight and the horizontal stress components depends only on the physical parameters of the

material, to be more precise it depends only on the angle of the shear resistance of the material.

Since that angle Φ changes as a function of the depth; the cos Φ can be expressed from the relation $tg\Phi = tg\varphi + \frac{c}{h\gamma \cdot \cos\Phi}$:

$$\sin\Phi = tg\varphi \cdot \cos\Phi + \frac{c}{h\gamma},$$

$$\sqrt{1-\cos^2\Phi} = tg\varphi \cdot \cos\Phi + \frac{c}{h\gamma},$$

$$\cos^2\Phi + tg^2\varphi \cdot \cos^2\Phi + \frac{2c}{h\gamma} tg\varphi \cdot \cos\Phi + \frac{c^2}{h^2\gamma^2} - 1 = 0$$

$$\cos\Phi = \frac{-\frac{c}{h\gamma} tg\varphi \pm \sqrt{tg^2\varphi + 1 - \frac{c^2}{h^2\gamma^2}}}{tg^2\varphi + 1},$$

since $$1 + tg^2\varphi = \frac{1}{\cos^2\varphi},$$

so

$$\cos\Phi = -\frac{c}{h\gamma}\sin\varphi \cdot \cos\varphi \pm \cos\varphi\sqrt{1 - \frac{c^2}{h^2\gamma^2}\cos^2\varphi},$$

respectively

$$\cos\Phi = \frac{\cos\varphi}{h\gamma}\left[\sqrt{h^2\gamma^2 - c^2 \cdot \cos^2\varphi} - c \cdot \sin\varphi\right].$$

Substituting the relation obtained for the cos Φ into the formula σ_x the horizontal component of the static pressure is:

$$\sigma_x = \frac{\cos\varphi}{2}\left[\sqrt{h^2\gamma^2 - c^2 \cdot \cos^2\varphi} - c \cdot \sin\varphi\right].$$

The horizontal stress components σ_x have a negative sign till a certain depth h_0. In the depth h_0 the value of the σ_x is 0. The depth of σ_x=0 can be expressed:

$$\frac{\cos\varphi}{2}\left[\sqrt{h_0^2\gamma^2 - c^2 \cdot \cos^2\varphi} - c \cdot \sin\varphi\right] = 0,$$

$$h_0^2\gamma^2 - c^2 \cdot \cos^2\varphi = c^2 \cdot \sin^2\varphi,$$

$$h_0^2\gamma^2 = c^2\left(\sin^2\varphi + \cos^2\varphi\right),$$

$$h_0 = \frac{c}{\gamma}.$$

Up to the depth h_0 the horizontal-surface cohesive granular material stands also without support in the vertical wall.

The value of the resultant force E_0 acting on the *h* high vertical retaining wall can be obtained by means of the definite integral of the horizontal stress components σ_x, taken from the depth h_0 to *h* (if on the retaining wall no friction develops, which according to the model experiments occurs as a result of rest):

$$E_0 = \int_{h_0}^{h} \sigma_x dh .$$

The result of the integration:

$$E_0 = \left[\frac{h}{4} \cos\varphi \sqrt{h^2\gamma^2 - c^2 \cdot \cos^2\varphi} - \frac{ch}{2} \sin\varphi \cdot \cos\varphi \right]_{h_0}^{h} -$$

$$- \left[\frac{c^2}{4\gamma} \cos^3\varphi \cdot \ln \left| \frac{h\gamma}{c \cdot \cos\varphi} \pm \sqrt{\frac{h^2\gamma^2}{c^2 \cdot \cos^2\varphi} - 1} \right| \right]_{h_0}^{h}$$

The term containing the ln can be left out because it is the third power of the cos φ, which is smaller than 1, and due to the fact that product of ln has a relatively small value , thus

$$E_0 \approx \frac{h \cdot \cos\varphi}{4} \sqrt{h^2\gamma^2 - c^2 \cdot \cos^2\varphi} - \frac{c}{4} \sin\varphi \cdot \cos\varphi \left(2h - \frac{c}{\gamma} \right).$$

Consequently, the resultant force of the static pressure of the horizontal-surface cohesive granular material, acting on the vertical retaining wall is :

$$\boxed{E_0 = \frac{h \cdot \cos\varphi}{4} \left[\sqrt{h^2\gamma^2 - c^2 \cdot \cos^2\varphi} - \left(2c - \frac{c^2}{h\gamma} \right) \sin\varphi \right].}$$

Inclination angle of the free slope

The angle Φ of the straight line linking a given point of the Coulomb's straight-line characteristic of the cohesive granular material and the origin, to the axis σ_n characterises the shear strength of the material in the depth belonging to the given

normal stress σ_n as the friction angle φ characterizes the non-cohesive granular material. The only difference can be discerned in the fact, that in the cohesive material this angle changes depending on the normal stress acting on the sheared surface. The tangent of the angle Φ can be expressed as a function of the depth in the following way:

Starting from the previously written relation $tg\Phi = tg\varphi + \frac{c}{h\gamma \cdot \cos\Phi}$ and

substituting $\cos\Phi = \sqrt{\frac{1}{1+tg^2\Phi}}$

$$tg\Phi = tg\varphi + \frac{c \cdot \sqrt{1+tg^2\Phi}}{h\gamma},$$

from which relation the tg Φ can be expressed:

$$\left(c^2 - h^2\gamma^2\right)tg^2\Phi + 2h^2\gamma^2 tg\varphi \cdot tg\Phi - \left(h^2\gamma^2 tg^2\varphi - c^2\right) = 0,$$

$$tg\Phi = \frac{h^2\gamma^2 tg\varphi \pm c\sqrt{h^2\gamma^2 tg^2\varphi + h^2\gamma^2 - c^2}}{h^2\gamma^2 - c^2},$$

$$tg\Phi = \frac{h^2\gamma^2 \cdot \sin\varphi \pm c \cdot \sqrt{h^2\gamma^2 - c^2 \cdot \cos^2\varphi}}{\cos\varphi(h^2\gamma^2 - c^2)}.$$

Taking into consideration, that in the cohesive granular materials, in a state of rest, the direction of the stresses rising from the self-weight inclines at an angle bigger than Φ to the horizontal; the biggest inclination angle of the free slope is determined by those stresses, which are produced by the vertical stresses rising from the self-weight, inclining at an angle Φ to the horizontal, which just do not exceed yet the side of the slope.

The cohesive slope can be constructed from the shear straight-line as follows (Figure 27):

After taking up the Coulomb's straight-line on the basis of the shear experiments, we can draw angle Φ, which changes depending on the depth: the angle of the internal shear resistance corresponding to point *A* of the Coulomb's straight-line is Φ_A. In the triangle *OAD* the side length *OD* is $h\gamma \cdot \cos\Phi_A$, i.e. it is the component of the vertical stress rising from the self-weight, perpendicular to the direction Φ_A. Consequently, the hypotenuse of the triangle *OA* is *hγ*, so taking the hypotenuse into the span of the compass, we get point *A'* by turning down the hypotenuse to the axis

$h\gamma$ starting vertically from point O, to which point the angle Φ_A is copied. Constructing the angles Φ belonging to the points taken up on the Coulomb's straight-line onto the straight line $h\gamma$ in this way, the envelope curve of the stress directions can be drawn. If the scale is divided by γ on the axis $h\gamma$, then we can obtain the geometric shape of the steepest slope of the horizontal-surface cohesive granular material.

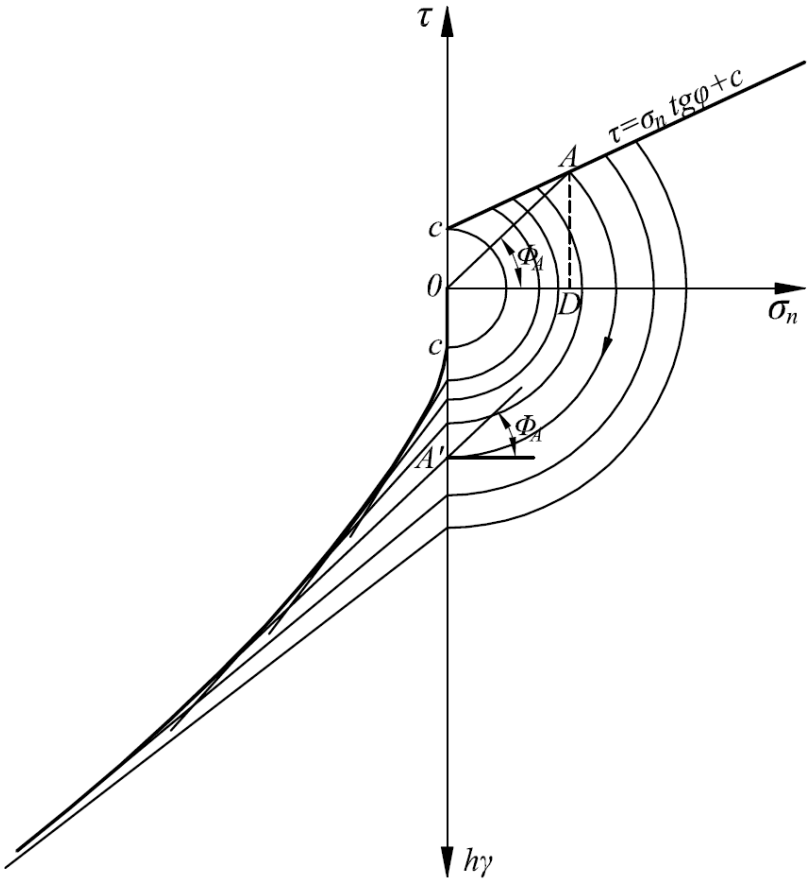

Figure 27. Constructing the cohesion slope

As far as the height $\frac{c}{\gamma}$ the cohesive granular material stands without support in a vertical wall, while the angle Φ is reduced by the increase of the depth, and goes towards the friction angle φ, as a limit. The shape of the steepest slope is of hyperbolic character. If the determination of the inclination angle of the steepest, but flat-surface slope, in proportion to the horizontal is the task, then the inclination angle β of the straight line connecting the given point of the envelop curve of the stress directions - which curve inclines to the horizontal at an angle Φ – to the O origin, as a flat slope side to the horizontal, determines inclination angle of the

chosen slope. Constructing the envelope curve of the stress directions inclining to the horizontal at an angle Φ by the help of the axis h - just directed over it (Figure 28) - , and starting from the origin *O,* the height belonging to the point cut on the envelope curve by the leg of a requested angle β provides the slope height, where under a slope angle β, and in case of a flat slope side the horizontal-surface cohesive granular material is still capable of standing without support.

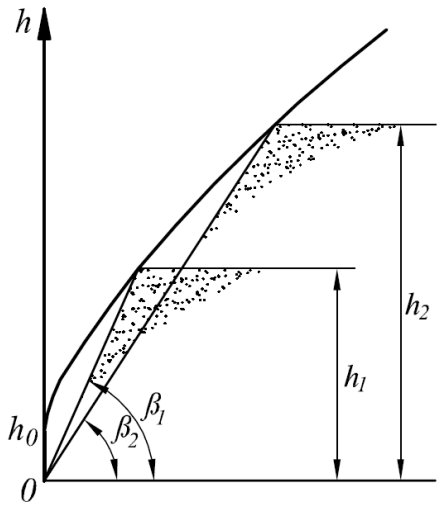

Figure 28. Relation between the slope height and slope angle

The envelope curve of the Φ stress directions has a concave character (Figure 27). The side of the slope can be flat (Figure 28), but convex as well. The extent of the convexity depends on the requirement that the stress directions examined on a vertical plane laid through any point of the slope, changing as a function of the depth, inclining at an angle Φ to the horizontal should not intersect the side of the slope. The convex envelope curve of the slope with a given height h_x can be constructed according to Figure 29:

The concave envelope curve is constructed by the method shown in Figure 27. The geometric shape of the h_x high concave slope is described by point *B* cut from the envelope curve by the horizontal line drawn from the point h_x and by the curve between h_0 *O*. The convex slope belonging to the height h_x can be obtained by

turning of the curve Oh_0B in such way that the positions of the points *O* and *B* are exchanged.

It is easy to prove by means of construction that in case of a convex slope the base point *B* is a stress-collecting place; therefore, the stability of the convex slope is less certain than the concave slope. Furthermore it is well discernible from the construction that the inclination angle of the straight line segment *OB,* measured to the horizontal, is at the same time, the biggest inclination angle β of the flat-surface slope belonging to the height h_x .

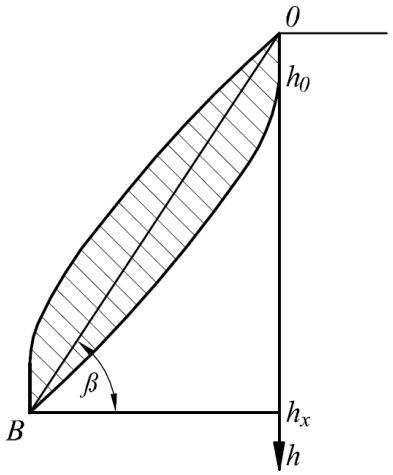

Figure 29. Constructing the convex slope

In Figure 29 in the part stripped between the geometrical slopes of the free slope with convex and concave boundary states, of height h_x , the geometric shape of the side of the slope can be so chosen that - assuming a continuous curve –that above the section *OB* it should show a convex character, below it a concave one. In case of a broken-line slope the examination must be performed for the Φ direction stresses depending on the depth, in order to prevent the stress directions from intersecting the side of the slope.

The formation of a slope with a convex boundary position can be expected, if the, for example, vertical wall supporting the material is removed carefully moving

downwards, while the slope with a concave boundary position can be obtained by removing the wall vertically upwards.

Active stress state

Inside the non-cohesive granular material the horizontal component of the active pressure is expressed by means of the following relation

$$\sigma_x = \frac{h\gamma}{2} tg\left(45^0 - \frac{\varphi}{2}\right)$$

In the cohesive granular material the following equation can be written for the horizontal component of the active stress – on the basis of the analogy of the Φ and the φ pertaining to the non-cohesive material, which occurs in a granular material with small friction angle and low cohesion already in relatively small depth –:

$$\sigma_x = \frac{h\gamma}{2} tg\left(45^0 - \frac{\Phi}{2}\right),$$

that is

$$\sigma_x = \frac{h\gamma}{2} \frac{1-\sin\Phi}{\cos\Phi}.$$

The values of the *sin*Φ and *cos*Φ can be expressed by means of the relation obtained from the Coulomb's straight-line:

$$tg\Phi = tg\varphi + \frac{c}{h\gamma \cdot \cos\Phi},$$

$$\sin\Phi = tg\varphi \cdot \cos\Phi + \frac{c}{h\gamma},$$

$$\cos\Phi = \frac{\sin\Phi}{tg\varphi} - \frac{c}{h\gamma \cdot tg\varphi}.$$

Substituting the values of the *sin*Φ and *cos*Φ into the relation written for σ_x:

$$\sigma_x = \frac{h\gamma}{2} tg\varphi \frac{h\gamma - h\gamma \cdot tg\varphi \cdot \cos\Phi - c}{h\gamma \cdot \sin\Phi - c},$$

but $$h\gamma \cdot \sin\Phi = h\gamma \cdot tg\varphi \cdot \cos\Phi + c,$$

so $$\sigma_x = \frac{h\gamma}{2}\left[\frac{h\gamma - c}{h\gamma \cdot \cos\Phi} - tg\varphi\right].$$

For the *cos*Φ we were able to deduce the following from the Coulomb straight-line:

$$\cos\Phi = \frac{\cos\varphi}{h\gamma}\left[\sqrt{h^2\gamma^2 - c^2 \cdot \cos^2\varphi} - c \cdot \sin\varphi\right].$$

Substituting the value of the *cos*Φ into the relation σ_x, the horizontal stress component of the active pressure developing inside the material in a given depth is:

$$\sigma_x = \frac{h\gamma}{2\cos\varphi}\left[\frac{h\gamma - c}{\sqrt{h^2\gamma^2 - c^2\cos^2\varphi - c \cdot \sin\varphi}} - \sin\varphi\right].$$

If the active stress condition is caused by the displacement – tilting – of the vertical and friction retaining wall, then the friction developed between the retaining wall and the material modifies the direction and magnitude of the stresses acting on the retaining wall.

The friction developed between the cohesive granular material and the wall are generally composed of the friction factor $tg\delta$ depending on the normal stress acting on the surface and the adhesion a independent of that, which is – in accordance with Coulomb's friction law – can be illustrated as it is shown in Figure 30.

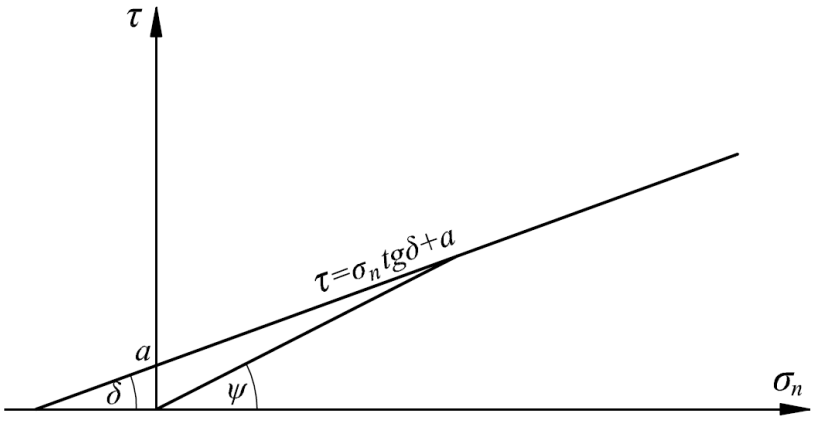

Figure 30. Friction developed between the cohesive granular material and the wall

At a given normal stress σ_n its friction angle is ψ. On the basis of Figure 30 the $tg\psi$ can be expressed:

$$tg\psi = \frac{\tau}{\sigma_n},$$

$$tg\psi = tg\delta + \frac{a}{\sigma_n}.$$

In the cohesive granular material the vertical stresses rising from the self-weight generate the Φ direction stresses.

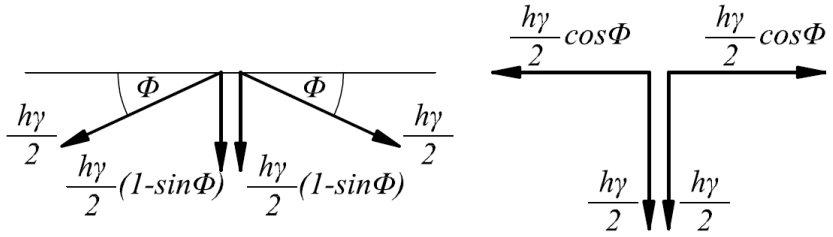

Figure 31. Cohesion stress model

Applying the stress model set up for non-cohesive granular materials to the cohesive material, and using Φ instead of the angle φ (Figure 31) – the relation of proportionality between the vertical and horizontal stress components can be written:

$$\frac{\sigma_y}{\sigma_x} = \frac{\frac{h\gamma}{2}}{\frac{h\gamma}{2}\cos\Phi}.$$

Next to a friction retaining wall, part of the vertical stress components of the cohesive granular material are transferred onto the retaining wall; on the retaining wall a weight-force intake realizes. If a stress σ_ψ acts on the retaining wall inclining at an angle ψ to the horizontal, then the retaining wall takes up a vertical-direction stress $\sigma_\psi \sin\psi$ from the material, i.e. reduces the vertical stress of the material part next to the retaining wall by $\sigma_\psi \sin\psi$. Therefore the horizontal stress component is also reduced proportionally. At the same time a $\sigma_\psi \cos\psi$ size horizontal stress component acts on the retaining wall the. On the basis of the proportion between the vertical and horizontal stress components it can be written:

$$\frac{\frac{h\gamma}{2}}{\frac{h\gamma}{2}\cos\Phi} = \frac{\frac{h\gamma}{2} - \sigma_\psi \sin\psi}{\sigma_\psi \cos\psi}.$$

The σ_ψ can be expressed:

$$\sigma_\psi = \frac{h\gamma}{2}\frac{\cos\Phi}{\cos\psi + \sin\psi \cdot \cos\Phi}.$$

The horizontal component of the σ_ψ is σ_h:

$$\sigma_h = \sigma_\psi \cos\psi,$$

$$\sigma_h = \frac{h\gamma}{2}\frac{\cos\Phi}{1 + tg\psi \cdot \cos\Phi}.$$

In the relation written for the $tg\psi$ in case of a vertical retaining wall $\sigma_n = \sigma_h$, so

$$\sigma_h = \frac{h\gamma}{2}\frac{\cos\Phi}{1 + tg\delta \cdot \cos\Phi + \frac{a \cdot \cos\Phi}{\sigma_h}}.$$

The σ_h can be expressed:

$$\boxed{\sigma_h = \frac{\cos\Phi}{2} \cdot \frac{h\gamma - 2a}{1 + tg\delta \cdot \cos\Phi}},$$

where

$$\cos\Phi = \frac{\cos\varphi}{h\gamma}\left[\sqrt{h^2\gamma^2 - c^2 \cdot \cos^2\varphi} - c \cdot \sin\varphi\right].$$

The active pressure of the cohesive granular material, acting on the friction retaining wall is, consequently, lower than its static pressure. If adhesion develops on the retaining wall the horizontal stress components are reduced by the following value

$$\frac{a \cdot \cos\Phi}{1 + tg\delta \cdot \cos\Phi}$$

as compared to the retaining wall without adhesion. The horizontal E_h component of the active compressive force of the cohesive granular material, acting on the retaining wall can be calculated by means of the definite integral of the σ_h, where the lower limit of the integration is given from the condition $\sigma_h = 0$:

$$\frac{\cos\Phi}{2}\cdot\frac{h\gamma-2a}{1+tg\delta\cdot\cos\Phi}=0.$$

The equality exists, if $\Phi=90^0$, which happens at $h_0=\frac{c}{\gamma}$, respectively if $h\gamma=2a$

and so $h=\frac{2a}{\gamma}$, that is $h_0=\frac{2a}{\gamma}$.

Consequently, the lower limit of the integration is h_0, but for h_0 the higher value must be taken into account from $\frac{c}{\gamma}$ and $\frac{2a}{\gamma}$

$$E_0=\int_{h_0}^{h}\frac{\cos\Phi}{2}\cdot\frac{h\gamma-2a}{1+tg\delta\cdot\cos\Phi}dh$$

where the $\cos\Phi$ is also the function of the *h*.

Summary

The basic physical properties of the granular material differ significantly from those of the chemically identical materials, which are, however in the solid, liquid or gaseous state, therefore, the definition of granular material as an additional state of matter in its own right is justified.

The ideal granular material is – similarly to the concept of perfect gas, ideal liquid and crystalline solid – a non-cohesive granular material.

The basic physical-mechanical laws of the non-cohesive granular materials are as follows:

I. In the non-cohesive granular materials only compressive and shear stresses can arise.

II. In the non-cohesive granular materials in a quiescent state, the stresses developed by the vertical-direction compressive stresses act downwards in the $\pm 90^0 - \varphi$ zone measured from the vertical direction. (φ is the angle of friction of the material.)

III. The value of the lateral pressure rising from the self-weight of the non-cohesive granular material is ($\frac{h\gamma}{2}$), i.e. the half of the product of the depth (h) and volume weight (γ), its direction deviates from the horizontal downwards with the angle of friction rising in the material, if the surface is horizontal and

over the given depth the material fills the space evenly inclining at an angle φ to the horizontal.

IV. The non-cohesive granular materials conforms to the physical-mechanical laws characteristic of them until their constituting elements, the grains keep their relative quiescent state. When the grains get into relative motion – collide with each other -, the granular materials behave according to the physical-mechanical laws of the liquids.

The physical-mechanical laws of the non-cohesive granular materials prevail with a statistical character, because the material itself consists of a multitude of different grains.

The stresses – the average forces calculated for a given surface – can be divided or compounded as vectors.

The factor of the static pressure is: $\lambda = \frac{\cos\varphi}{2}$.

In the non-cohesive granular material, the lateral pressure — in a plane inclining at an angle β to the horizontal and tilting towards the assembly — is $\sigma_{\varphi} = \frac{h\gamma}{2}\left(1 - \frac{tg\varphi}{tg\beta}\right)$ and its direction inclines at an angle φ to the horizontal.

In the active stress condition arising due to the expansion, the motion is realised in the direction of $45^0 + \frac{\varphi}{2}$ to the horizontal.

The horizontal component of the pressure acting on the vertical friction retaining wall is $\sigma_h = \frac{h\gamma}{2} \cdot \frac{\cos\varphi}{1 + tg\delta \cdot \cos\varphi}$, where δ is the angle of friction developed between the retaining wall and the material.

The simultaneous existence of two equalities in a trough formulates the condition of the arch formation:

$$\frac{b}{h} \le \lambda \cdot tg\varphi ,$$

$$\frac{b}{h} \le \lambda \cdot tg(\beta + \delta) - tg\beta ,$$

where:

b is the size of the discharge orifice of the trough,

h is the height of the trough,

λ is the factor of the static pressure,

β is the inclination angle of the trough, measured to the vertical,

δ is the angle of the friction developed between the trough and the material.

The discharge from the trough can occur by mass flow, if $\alpha \rangle \beta + \delta$, that is $\frac{b}{h} \rangle \lambda \cdot tg(\beta + \delta) - tg\beta$. The tunnel flow occurs, if $\alpha \langle \beta + \delta$, that is $\frac{b}{h} \langle \lambda \cdot tg(\beta + \delta) - tg\beta$, but $b \rangle \lambda h \cdot tg\varphi$.

The geometric equation of the arch is $y = \left(\frac{b}{4} - \frac{x^2}{b} \right) \frac{b + h \cdot tg\beta}{\lambda h}$, and $y = \left(\frac{b}{4} - \frac{x^2}{b} \right) tg(\varepsilon + \varphi)$, if the arch is supported by the material in the plane inclining at an angle ε to the vertical. The angle ε can be calculated.

Flow-proof hoppers can be designed in the knowledge of the conditions of the formation of the arch. The present work shows the procedure of the design. The experiment carried out with use of the curve-component hopper, received with this design procedure, proved the correctness of the theoretical calculations.

In the cohesive granular material of quiescent state the stresses produced by the vertical-direction compressive stresses act downwards in the zone $\pm 90^0 - \Phi$ measured from the vertical direction (where Φ is the angle of the internal shear resistance of the material).

The value of the static pressure of the cohesive granular material, rising from the self-weight, is half of the product of the depth and volume weight $\left(\frac{h\gamma}{2}\right)$, its direction deviates from the horizontal downwards by the angle of the internal shear resistance of the material. The horizontal stress component of the static pressure is:

$$\sigma_x = \frac{h\gamma}{2}\cos\Phi,$$

and

$$\sigma_x = \frac{\cos\varphi}{2}\left[\sqrt{h^2\gamma^2 - c^2\cdot\cos^2\varphi} - c\cdot\sin\varphi\right],$$

where the c is the cohesional coefficient.

The resultant force of the static pressure of the horizontal-terrain cohesive granular material, acting on the vertical retaining wall is:

$$E_0 = \frac{h\cdot\cos\varphi}{4}\left[\sqrt{h^2\gamma^2 - c^2\cdot\cos^2\varphi} - \left(2c - \frac{c^2}{h\gamma}\right)\sin\varphi\right].$$

The cohesive granular material in a vertical wall without support is stable until the height

$$h_0 = \frac{c}{\gamma}$$

The basic principle of the construction of the steepest slope is that the Φ-direction stresses developed by the self-weight should touch the side of the slope. The procedure of the construction of the cohesive slope can be found in the present work.

The horizontal stress component of the active pressure of the cohesive granular material, acting on the vertical retaining wall having a friction angle δ and and adhesion coefficient a is:

$$\sigma_h = \frac{\cos\Phi}{2}\cdot\frac{h\gamma - 2a}{1 + tg\delta\cdot\cos\Phi},$$

where

$$\cos\Phi = \frac{\cos\varphi}{h\gamma}\left[\sqrt{h^2\gamma^2 - c^2\cdot\cos^2\varphi} - c\cdot\sin\varphi\right].$$

Bibliography

1. Mester, L.: Kohézió nélküli szemcsés anyagok fizikai-mechanikai elméletének alapjai. (The Basic physical-mechanical theory for noncohesive granular materials) Akadémiai Kiadó, Budapest, 1977. 39p.
2. Mester, L.: Kohézió nélküli szemcsés anyagok fizikai-mechanikai alaptörvényei. (Basic physical-mechanical laws of the noncohesive granular materials) Járművek, Mezőgazdasági Gépek, 1977. 24.3. 109-114p.
3. Mester, L.: Szemcsés anyagok fizikai-mechanikai tulajdonságai. (The physical-mechanical properties of the granular materials) Tanulmány. Mezőgépfejlesztő Intézet, 1977. 83p.
4. Mester, L.: Feszültségek a kohéziós szemcsés anyagokban. (Stresses in cohesive granular materials) Járművek, Mezőgazdasági Gépek, 1978. 25.2. 56-60p.
5. Mester, L.-Czike, I.: Mezőgazdasági szemes és szemcsés anyagok agrofizikai jellemzőinek meghatározása. (Determination of the agrophysical characteristics of agricultural granular materials) Élelmezési Ipar, 1979. 33.9. 349-355p.
6. Mester, L.: A boltozat kialakulásának mechanizmusa szemcsés anyagokban, a garatméretezés elméleti alapjai. (The mechanism of the arch formation in granular materials, basic principles of the hopper design) Járművek, Mezőgazdasági gépek, 1980. 27.8. 285-290p.
7. Mester, L.-Tóth, F.: Folyásjavító garatok szemcsés anyagok silós tárolásához. (Hoppers with flow-improving features for silo storage of the granular materials) Mezőgazdasági Technika, 1980. 20.12. 26p.
8. Terzaghi, K.: Large Retaining Wall Tests, Engg, News Record No.112. 1934.
9. Terzaghi, K.: Stress Distrubution in Dry and in Saturated Sand above a Yielding Trap- Door. Proc. Inf. Comf. Soil Mech. I. Camdridge 1936.